# What Matters in Hierarchical Search for Solving Combinatorial Problems?

**Anonymous authors**
**Paper under double-blind review**

## Abstract

Combinatorial problems, particularly the notorious NP-hard tasks, remain a significant challenge for AI research. A common approach to addressing them combines search with learned heuristics. Recent methods in this domain utilize hierarchical planning, executing strategies based on subgoals. Our goal is to advance research in this area and establish a solid conceptual and empirical foundation. Specifically, we identify the following key obstacles, whose presence favors the choice of hierarchical search methods: *hard-to-learn value functions, complex action spaces, presence of dead ends in the environment,* or *training data collected from diverse sources*. Through in-depth empirical analysis, we establish that hierarchical search methods consistently outperform standard search methods across these dimensions, and we formulate insights for future research. On the practical side, we also propose a consistent evaluation guidelines to enable meaningful comparisons between methods and reassess the state-of-the-art algorithms.

## 1 Introduction

The ability to solve discrete tasks that require sophisticated reasoning, particularly those involving NP-hard problems, is essential for advancing AI (Bengio et al., 2021). These include complex problems like theorem proving (Wu et al., 2021; Trinh et al., 2024), constraint satisfaction problem (Achiam et al., 2017), molecule alignment (Needleman & Wunsch, 1970; Smith & Waterman, 1981), social network analysis (Kipf & Welling, 2017), or navigation (LaValle, 2006; Choset et al., 2005).

Even driving a car, which typically involves continuous control of steering and speed, requires high-level discrete decision-making, e.g., when to overtake, when to change lanes, or how to navigate through traffic (Kiran et al., 2022).

Addressing that kind of tasks, known as combinatorial problems, requires efficient planning strategies due to the vast and complex search spaces involved (Bruck & Goodman, 1987). A promising approach to this challenge, inspired by how humans plan their actions (Hull, 1932; Fishbach & Dhar, 2005; Kool & Botvinick, 2014), is hierarchical search. This general-purpose method breaks down a problem into manageable subproblems, or subgoals, making the overall task more tractable, in contrast to low-level meth-

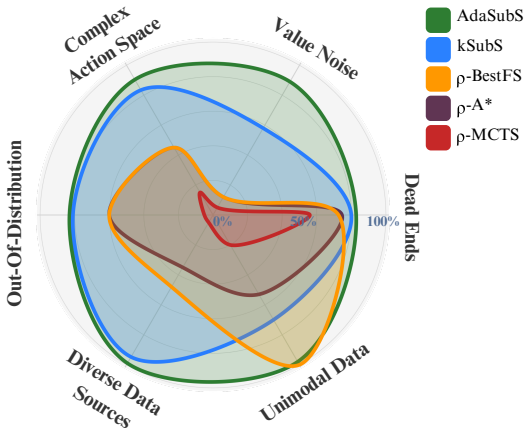


Figure 1: Schematic performance comparison of hierarchical methods (AdaSubS, kSubS) and low-level methods ($\rho$-BestFS, $\rho$-A*, $\rho$-MCTS) across six dimensions: *handling data collected from diverse sources*, *learning from clean unimodal demonstrations*, *avoiding dead ends*, *performance under high value approximation errors*, *handling complex action space*, and *generalizing to out-of-distribution instances*.

ods that rely on atomic actions for planning. Hierarchical
search has been successfully applied to a variety of combinatorial tasks, as evidenced by methods like Subgoal Search (kSubS) (Czechowski et al., 2021), and further advanced by approaches such as Adaptive Subgoal Search (AdaSubS) (Zawalski et al., 2023), Hierarchical Imitation Planning with Search (HIPS) (Kujanpää et al., 2023a), and HIPS-$\varepsilon$ (Kujanpää et al., 2023b).

Our goal in this paper is to advance research in hierarchical planning and establish a solid conceptual and empirical foundation. We identify four key challenges whose presence highly favors the use of hierarchical search methods: *hard-to-learn value functions, complex action spaces, presence of dead ends in the environment, or data collected from diverse sources*. Through comprehensive empirical analysis, we demonstrate that hierarchical methods consistently outperform standard search techniques in overcoming these critical obstacles. Furthermore, we propose a consistent evaluation methodology to facilitate meaningful comparisons between methods and reassess current state-of-the-art algorithms. Our findings offer a clearer understanding of when hierarchical approaches should be preferred over low-level methods.

In summary, our contributions are as follows:

- We present a comprehensive empirical analysis comparing the performance of hierarchical search methods against low-level search methods across diverse problem settings.
- We identify problem characteristics that influence performance, providing insights into when hierarchical methods should be favored over low-level methods.
- We propose a standardized evaluation guidelines that facilitate meaningful and consistent comparisons across different types of search methods.

## 2 Related Work

**Solving Decision-Making Problems** Decision-making problems are often framed as Markov Decision Processes (MDPs) (Sutton et al., 1999), which can be solved using Reinforcement Learning (RL) algorithms like PPO (Schulman et al., 2017) or DQN (Mnih et al., 2015). These methods learn policies through interaction with the environment. An alternative to learning from trial and error is Imitation Learning (IL), training models directly from offline demonstrations. The availability of large-scale datasets (Walke et al., 2023; Collaboration et al., 2023; Grauman et al., 2022; Dosovitskiy et al., 2017), make it applicable to the most complex domains like robotics (Mandlekar et al., 2018; Edmonds et al., 2017; Kim et al., 2024), autonomous driving (Kelly et al., 2019; Li et al., 2022; Zhang & Cho, 2017), and physics-based control (Kim et al., 2020; Fickinger et al., 2022). Key foundational methods such as Behavioral Cloning (BC) (Sutton & Barto, 1998), Inverse Reinforcement Learning (IRL) (Baker et al., 2009), or DAgger (Ross et al., 2011) have been instrumental in advancing IL for complex environments where direct exploration is less practical. In this work, we use IL to train components for the search methods, such as the policy and value function, which is a widely adopted approach (Czechowski et al., 2021; Zawalski et al., 2023; Takano, 2023).

**Subgoal Methods** Hierarchical Reinforcement Learning methods tackle complex decision-making tasks by breaking them into subgoals. HIRO (Nachum et al., 2018) reuses past data by goal relabeling. HAC (Levy et al., 2019) builds a multi-layer hierarchy of policies trained with hindsight. Hierarchical Diffuser (Chen et al., 2024) learns to predict future states with diffusion models. Graph-based methods, such as SoRB (Eysenbach et al., 2019) or DHRL (Lee et al., 2022) build a high-level graph of states, which then allow for efficient shortest path finding. GCP (Pertsch et al., 2020) learns to predict middle states between two given observations. Algorithms such as HPG (Ghavamzadeh & Mahadevan, 2003) or H-DDPG (Yang et al., 2018) extend the classical RL algorithms to the hierarchical setting.

In the area of combinatorial problems, there has been growing interest in applying HRL techniques. kSubS (Czechowski et al., 2021) introduces a hierarchical search algorithm that iteratively generates subgoals to construct a search tree. Building on this, AdaSubS (Zawalski et al., 2023) incorporates multiple subgoal generators, each trained to predict subgoals at different distances from the target, allowing for dynamic

adaptation of the planning horizon based on problem complexity. HIPS (Kujanpää et al., 2023a) and HIPS-$\varepsilon$ (Kujanpää et al., 2023b) perform search using subgoals generated by VQ-VAE models (van den Oord et al., 2017).

**Low-level Search Algorithms** Traditional search algorithms like Best-First Search (BestFS), A* (Cormen et al., 2009; Russell & Norvig, 2009), and Monte Carlo Tree Search (MCTS) (Veness et al., 2009; James et al., 2017) have long been the foundation for solving complex decision-making problems. Recent advancements have improved these methods by integrating neural network-based heuristics, improving their efficiency in large search spaces (Silver et al., 2018; Yonetani et al., 2021). A variant of $\rho$-BestFS used in (Czechowski et al., 2021; Zawalski et al., 2023), leverage heuristics learned through behavioral cloning to guide search. More recent algorithms, like PHS (Orseau & Lelis, 2021) or LevinTS (Orseau et al., 2023), combine policy-driven and value-based approaches, offering both theoretical guarantees and strong empirical performance. Additionally, PDDL planners (Haslum et al., 2019) solve decision-making problems by using predefined action models and goals, with domain-independent planners offering broad applicability, while domain-specific ones achieve higher performance in specialized tasks.

**Empirical Studies on Algorithmic Performance** Our work aligns with recent empirical studies that investigate the conditions under which various algorithmic approaches excel. For instance, Andrychowicz et al. (2020) investigate how specific design choices influence the performance of PPO, while other research compares offline reinforcement learning with behavioral cloning (Kumar et al., 2022) or explores design choices for language-conditioned robotic imitation learning (Mees et al., 2022). In this paper, we focus on hierarchical search in combinatorial problems, specifically studying the conditions where hierarchical methods outperform low-level planners. To the best of our knowledge, this is the first systematic study of the relationship between hierarchical and low-level search in this context.

## 3 Combinatorial Environments

Our study targets solving combinatorial environments – domains with discrete, compact state representations corresponding to exponentially large configuration spaces, which makes them highly challenging to solve. This class includes several NP-hard problems, such as the Traveling Salesman Problem (Applegate et al., 2006), the Rubik's Cube (Singmaster, 1981), Sokoban (Culberson, 1997), or solving non-linear inequalities (Sahni, 1974). In our study, we specifically focus on goal-reaching tasks. To efficiently solve combinatorial problems an algorithm should have the following desirable properties:

In combinatorial environments, each problem instance is typically entirely distinct from others, making it unrealistic to assume that offline data provides comprehensive state space coverage. This is especially critical in problems like the Rubik's Cube, where even with a vast training dataset, any new state will be entirely different from those previously encountered. Some approaches rely on sufficient state space coverage, but in many combinatorial problems, this assumption is impractical.

1. **Learning from offline data.** Since combinatorial environments are characterized by a large space of possible configurations, learning without priors or handcrafted dense rewards is infeasible due to the challenge of exploration[1]. To address this, a canonical solution is to leverage offline data. Other possible approaches, such as clever reward shaping, usually require significant domain knowledge.

2. **Combinatorial space abstraction.** In combinatorial environments, each problem instance is typically entirely distinct from others. Hence, it is unrealistic to assume a comprehensive state space coverage by training data or repeated visits to nearby states, an assumption that some approaches implicitly rely on.

3. **Search.** Methods that don't use search and follow a single action trajectory are inherently limited by computational complexity, since they can perform only a constant number of operations before

[1]For instance, we tested PPO (Schulman et al., 2017) on the Rubik's Cube, but, unsurprisingly, it failed to make any progress due to never reaching the goal in the haystack of $4.3 \times 10^{19}$ states, hence never observing a positive reward.

choosing an action. Solving NP-hard problems within a fixed computation budget is computationally infeasible (Bruck & Goodman, 1987).

Many hierarchical methods have not been designed for combinatorial problems, so they fail to meet the listed conditions and cannot be expected to be efficient in these applications. For instance, Chen et al. (2024); Yang et al. (2018) require continuous state or action space, Ghavamzadeh & Mahadevan (2003) learns only from online interactions, Eysenbach et al. (2019); Huang et al. (2019); Lee et al. (2022) assume a good coverage of the whole state space, and Nachum et al. (2018); Levy et al. (2019) do not use planning to determine actions.

## 4 Subgoal Methods

Subgoal methods, or hierarchical methods, are a family of algorithms designed to solve complex decision-making tasks by breaking down the overall objective into smaller, more manageable subgoals (Sutton et al., 1999). Instead of searching for a sequence of low-level actions that directly lead from the initial state to the goal, the agent first identifies high-level intermediate targets – subgoals – that guide the trajectory toward the final goal. The use of subgoals is widely considered as a method that scales better to longer horizons (Chen et al., 2024; Lee et al., 2022), mitigates errors in value approximations (Czechowski et al., 2021), and reduces overall complexity by decomposing the problem into smaller subproblems (Sutton et al., 1999; Zawalski et al., 2023). The process of searching involves the following components:

- **Subgoal generator** that, given a state within the search tree, outputs a set of subgoals. For instance, a subgoal may be a future state (Czechowski et al., 2021; Zawalski et al., 2023) or a class of desired outcomes (Jiang et al., 2019; Panov & Skrynnik, 2018). See Figure 16 for example subgoals. The subgoal generator can be implemented using models such as transformers with beam search (Czechowski et al., 2021; Zawalski et al., 2023), VQ-VAE (Kujanpää et al., 2023a), or other generative architectures. The generator is used by the planner to construct a search tree of subgoals.

- **Low-level policy** that determines a path of low-level actions between subgoals. For instance, it may be a trained goal-reaching policy (Czechowski et al., 2021; Zawalski et al., 2023), a local search (Czechowski et al., 2021; Kujanpää et al., 2023a), or a stored path from previous episodes (Eysenbach et al., 2019; Lee et al., 2022).

- **Planner** that determines the order in which subgoals are generated. Standard planning algorithms like BestFS (Czechowski et al., 2021), PHS (Kujanpää et al., 2023a), or their modified forms (Zawalski et al., 2023), are typically used.

- **Value function** that estimates the distance between the given state and the goal state. The planner uses this information to select the next node to expand with the subgoal generator. In some works it is also called *heuristic value*.

In our experiments, we use kSubS (Czechowski et al., 2021) and AdaSubS (Zawalski et al., 2023) as subgoal methods well-suited for combinatorial problems, as they satisfy the conditions formulated in Section 3. We also experimented with HIPS and HIPS-$\varepsilon$ (Kujanpää et al., 2023a;b), but these methods generally fail to solve the problems within a reasonable computational budget. Therefore, their results are omitted from the main text and discussed in Appendix I.

We compare the performance of the selected subgoal approaches against three popular low-level methods: BestFS, A*, and MCTS. To ensure a fair comparison and improve efficiency, we augment these algorithms by using a trained policy to select the top actions before each node expansion. We refer to them as $\rho$-BestFS, $\rho$-A*, and $\rho$-MCTS. A detailed description, analysis, and pseudocode for each of these algorithms can be found in Appendix F. See also Appendix H for diagrams explaining different search methods.

### 4.1 Training Components

In our experiments, the models for both subgoal methods and low-level searches were trained using imitation learning, following standard practice (Nair et al., 2018; Czechowski et al., 2021). Specifically, we collected a dataset of approximately 500 000 trajectories for each environment. Trajectories are sequences of consecutive states and actions leading to the goal state. We used various methods of dataset collection, like hand-crafted algorithms, trained policies, reversed random shuffles, and others, which let us to study the influence of training data characteristics on the performance of search methods.

To ensure a fair comparison, all methods shared common components whenever applicable (e.g., each method uses the same value function). This allows us to focus on the differences between the search algorithms, rather than heuristic biases. No additional heuristics were used, ensuring that performance differences arise solely from the algorithmic approaches.

More details on training the components, including specific objectives, are provided in Appendix D.

### 4.2 Performance Metric

Our performance metric is the *success rate*, defined as the percentage of problem instances solved within a given *complete search budget*. The complete search budget is the total number of visited states in the search tree. In particular, for subgoal methods, the budget includes both the generated subgoals and the states visited by the low-level policy used to connect these subgoals.

By accounting for the total number of visited states, this metric provides a unified and fair comparison of search efficiency across different methods. We argue that reporting only the number of visited subgoal nodes would unfairly favor subgoal methods (see Appendix I for details).

## 5 Analysis

We investigate how environmental properties and training data influence the performance of hierarchical methods compared to low-level search approaches in combinatorial tasks. While previous works (Czechowski et al., 2021; Zawalski et al., 2023; Kujanpää et al., 2023a;b) show a considerable advantage of hierarchical methods, our experiments reveal that this advantage is not consistent across all scenarios (see Figures 4 or 5 for specific examples). Specifically, we answer the following research questions:

- Q1. Is hierarchical search more effective than low-level search for solving combinatorial problems?
- Q2. What environmental properties and characteristics of the training data amplify performance differences? When hierarchical search should be preferred over low-level search?
- Q3. What pitfalls should be avoided when interpreting experimental results?

To address these questions, we conducted a wide range of experiments comparing subgoal and low-level search algorithms across a variety of combinatorial tasks. Below, in each subsection we summarize the key findings that reveal the most significant factors affecting performance, followed by a brief discussion. For each finding, we link it to the relevant research questions. The extended analysis of these factors can be found in Appendix B.

We present our findings using the *Rubik's Cube, Sokoban, N-Puzzle*, and *Inequality Theorem Proving* (INT) (Wu et al., 2021) environments[2]. These classical benchmarks are widely used in planning research (McAleer et al., 2019; Czechowski et al., 2021) and are known to be NP-hard (Demaine et al., 2018; Culberson, 1997; Ratner & Warmuth, 1986). Detailed descriptions of these environments can be found in Appendix A.

All methods in our study were trained using imitation learning. In particular, all algorithms share the same value function, as stated in Section 4.1. To ensure fair comparisons, we measured complete search budgets, in

[2] We note that classical environments have domain-specific solvers that achieve high performance by relying on expert knowledge. However, our goal is to compare general-purpose search methods that require no domain knowledge.

contrast to counting only high-level search nodes, to avoid giving any unfair advantage to subgoal methods, as discussed in Section 4.2 (which contributes to the research question Q3). We tuned hyperparameters of each method separately for each experiment to ensure optimal performance.

### 5.1 Subgoal Methods are Robust to Diverse Sources of Data

Achieving superhuman performance in complex tasks often involves large-scale datasets of demonstrations obtained from agents with varying skill levels and strategies (Silver et al., 2016). By training models on data collected from a variety of solvers and testing them in the Rubik's Cube and N-Puzzle environments, we show that the variability in training data has a significant impact on the performance of search algorithms. Our training data included algorithmic solvers, computational solvers, and random shuffles, as detailed in Appendix B.1.

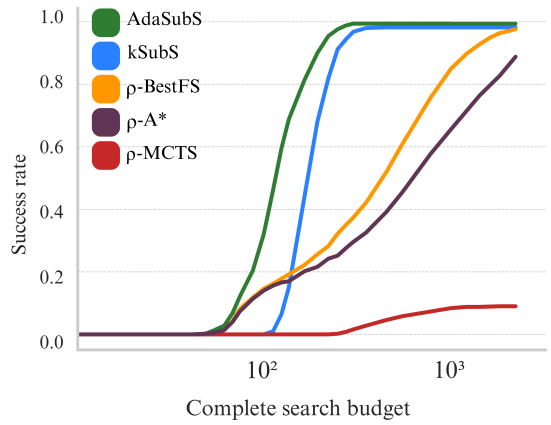


Figure 2: Solving the Rubik's Cube. Components are trained on data from 4 different solvers.

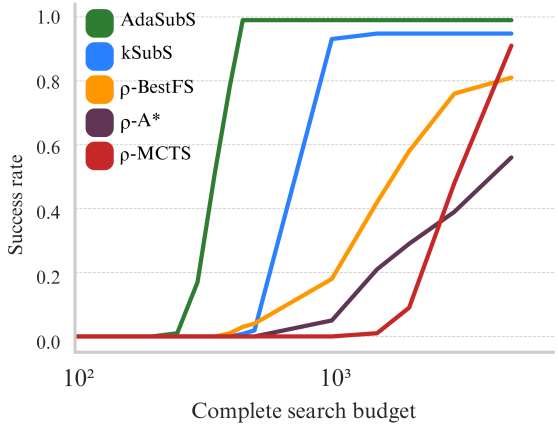


Figure 3: Solving the N-Puzzle. Components are trained on data from 2 different solvers.

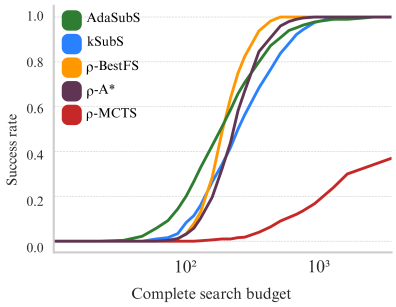


Figure 4: Solving the Rubik's Cube. Components are trained on reversed random shuffles.

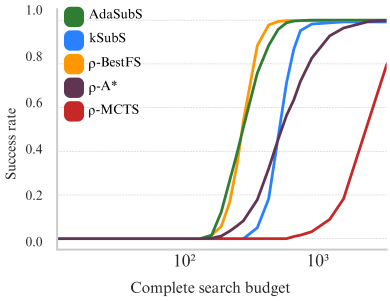


Figure 5: Solving the Rubik's Cube. Components are trained on the *Beginner* algorithmic solver.

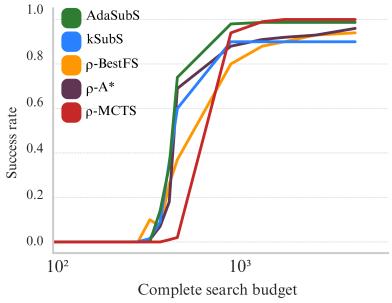


Figure 6: Solving N-Puzzle. Components are trained on an algorithmic solver.

As shown in Figures 2-3, subgoal methods consistently outperform low-level methods by a wide margin (Q1). However, when the training dataset is limited to a single source of demonstrations – whether the demonstrations are long and structured or short and direct – this performance gap disappears (see Figures 4-6). Notably, subgoal methods, particularly AdaSubS, maintain stable performance across all training setups, while low-level methods are highly sensitive to the characteristics of the training data.

To explain those results, we found that value functions trained on diverse data often fail to assign consistently low values to the initial states of tasks. When demonstrations differ significantly in their length or execution

style, the value function learns this variation, leading to inconsistent value predictions. Hierarchical methods can overcome this issue by relying on subgoals. Subgoals enable the agent to make long steps toward the solution, effectively bypassing regions of the state space where the value function is inconsistent or noisy, as it does not need to assess every small step along the way (this property is further studied in Section 5.2). In contrast, low-level methods operate on a finer, step-by-step level, executing small, atomic actions. This makes them more sensitive to the variability in the value function because they must evaluate each intermediate state on the way.

More detailed analysis of the experiments involving diverse data sources is provided in Appendix B.1.

**Takeaway** *Subgoal methods successfully leverage diverse demonstrations (Q2), while low-level search performs better when trained on homogeneous trajectories (Q2).*

### 5.2 Subgoal Methods are Value Noise Filters

We found that the classical search algorithms are highly sensitive to the quality of the value function. To show this in a controlled setting, we added Gaussian noise to the value estimates and observed how different noise levels impacted the success rate of solving tasks.

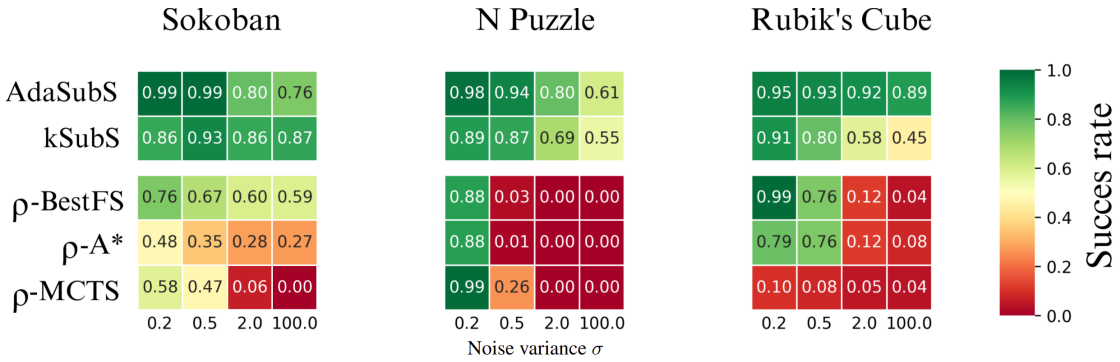


Figure 7: Success rate of low-level and subgoal methods as the approximation errors of the value function increase. $\sigma = 100$ results in completely random value estimates.

While $\rho$-BestFS is able to solve nearly all instances under ideal conditions, its performance significantly declines as value function errors increase, even to 0% (see Figure 7). $\rho$-A* and $\rho$-MCTS behave similarly. In contrast, the subgoal methods show remarkable resilience. Particularly AdaSubS, which maintains nearly unchanged success rate, despite high value errors (Q2).

These results align with our findings in Section 5.1, where using diverse training data naturally introduced value estimation errors. As observed by Zawalski et al. (2023), the search process of subgoal methods is guided by subgoal generators, which reduces reliance on the value function. Subgoal generators and the conditional policies connecting subgoals are not directly influenced by the value approximation errors. The value function is used only in high-level nodes, which represent only a fraction of the search tree.

In hierarchical methods, the distance between high-level nodes spans multiple steps, increasing the likelihood that value estimates for subsequent high-level nodes along the solution path will be monotonic (see Figure 8 for an illustrative example), which makes planning more efficient. This supports the claim by Czechowski et al. (2021) that subgoals effectively mitigate the impact of value noise. To further ground that result, we prove the following theorem:

**Theorem 1** (Search advancement formula)**.** *Let $g_k : S \to \mathcal{P}(S)$ be a stochastic $k$-subgoal generator that, given a state $s \in S$ samples a set of $b$ subgoals $\{s_i\}$ such that the distances $d(s_i, s)$ are independent, uniformly distributed in the interval $[-k; k]$. Let $V : S \to \mathbb{R}$ be a value function with approximation error uniformly distributed in the interval $[-\sigma; \sigma]$.*

*Then, after $n$ iterations of search, the expected total progress toward the goal is:*

$$\mathbb{E}_{Adv} = \frac{nb}{4\sigma k} \int_{-k}^{k} x \left( \int_{-\sigma}^{\sigma} \tilde{u}(x+h)^{b-1} \mathrm{d}h \right) \mathrm{d}x, \tag{1}$$

*where $\tilde{u}(x)$ is CDF of the sum of two uniform variables $U(-k,k)+U(-\sigma,\sigma)$. Additionally, if we approximate that sum as $U(-k-\sigma,k+\sigma)$, we get*

$$\mathbb{E}_{Adv} \approx \frac{n\left((k+\sigma)^b(bk^2+bk\sigma-2k\sigma-2\sigma^2)+\sigma^b(2k\sigma+bk\sigma+2\sigma^2)-k^b(bk^2)\right)}{(b+1)(b+2)k\sigma(k+\sigma)^{b-1}} \tag{2}$$

*Proof.* See Appendix K for the proof. □

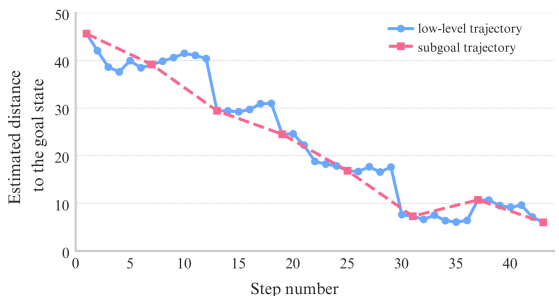


Figure 8: Value estimates along a solving trajectory generated by $\rho$-BestFS. Even small approximation errors cause non-decreasing values, slowing down the search. In contrast, the subgoal path mitigates these errors, leading to mostly monotonic values along the trajectory.

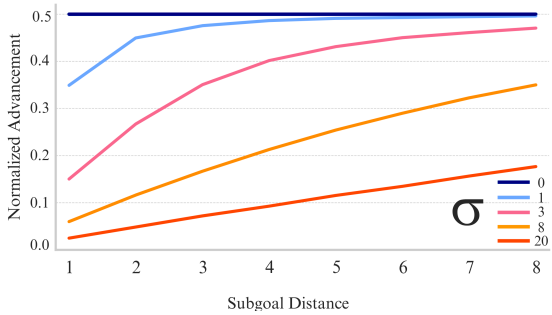


Figure 9: Normalized advancement $\mathbb{E}_{Adv}/k$ for a single search iteration, according to Theorem 1. The value for each subgoal is divided by its length to represent the advancement per atomic action for easier comparison.

Theorem 1 quantifies the expected progress of the search at each step, with Equation 1 giving an exact formula and Equation 2 providing a useful approximation. To compare subgoal methods with low-level methods in theory, under different levels of value approximation error, we model low-level search by setting $k = 1$, which represents a single action. Figure 9 shows the expected search progress with a branching factor of $b = 3$, normalized by the number of actions leading to a subgoal.

When value estimates are perfect (i.e., $\sigma = 0$), both subgoal and low-level searches perform similarly. However, as value approximation errors increase, subgoal methods become significantly more resilient. At high noise levels ($\sigma = 20$), single-step searches make very little progress, advancing only 0.025 per action. In contrast, subgoals of length 8 achieve much greater progress – 1.4 for the entire subgoal, which is 0.175 per action. This 7-fold increase in theoretical efficiency explains why subgoal methods outperform low-level methods in our experiments.

Further analysis of these experiments can be found in Appendix B.2.

**Takeaway** *Subgoal methods successfully handle value approximation errors. Thus, they should be used when estimating the value is hard, for instance, when learning from diverse and suboptimal demonstrations (Q2).*

### 5.3 Subgoal Methods Handle Complex Action Spaces

In environments with large action spaces, search methods often struggle due to the exponential increase in the number of choices (Sutton & Barto, 1998). As shown in Figure 10, subgoal methods demonstrate a clear advantage over low-level search methods in the INT environment (Wu et al., 2021), a benchmark

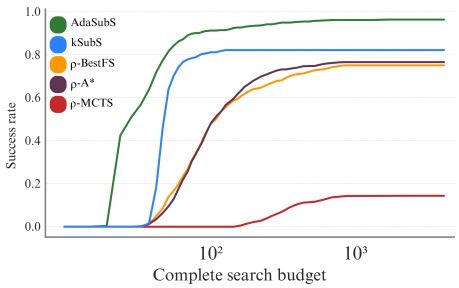


Figure 10: Solving INT. Components are trained on randomly generated proofs.

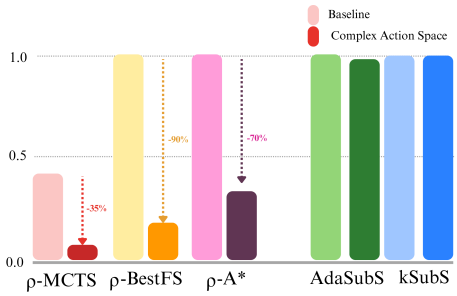


Figure 11: Solving the Rubik's cube with expanded action space, compared with the standard setup. Components are trained on reverse random shuffles.

on proving mathematical inequalities (Q1). The INT environment is particularly challenging because of its highly complex observation and action spaces, making it the most difficult benchmark among those used in (Czechowski et al., 2021; Zawalski et al., 2023; Kujanpää et al., 2023a;b).

Given a complex action space, each node expansion in low-level methods involves executing many similar actions, limiting their ability to efficiently search through the space. In contrast, subgoal methods compute actions only to connect subgoals, which is a much simpler task. This targeted approach reduces the negative impact of a large action space, allowing subgoal methods to maintain their efficiency even as the action space grows (Q2).

To confirm this explanation, we conducted experiments on a modified version of the Rubik's Cube, where the action space was artificially inflated by giving the agent access to 100 copies of each action. As shown in Figure 11, this simple modification drastically reduces the success rates of all low-level methods, even below 35%. In contrast, subgoal methods remain largely unaffected, performing similarly to the standard setup. We can explain that result with the following theorem:

**Theorem 2** (Densification of the action space)**.** *Fix any state $s$ from the state space $S$. Let $f : A \to [0, 1]$ be the action distribution induced by the data-collecting policy for the state $s$. Assume that $f$ is continuous and has a unique maximum.*

*For clarity, assume $A = [0, 1]$. Consider a sequence of increasingly dense discrete action spaces $A_n := \{i/n\}_{i=0}^{n} \subset A$. Let $\rho_n : S \times A_n \to [0, 1]$ be a family of policies that learn the distribution $f|_{A_n}$ over actions, with uniform approximation error $U(-E, E)$, where $E \in \mathbb{R}_+$. Let $r_n$ be the range of the top $K$ actions according to the probabilities estimated by $\rho_n$. Then*

$$\lim_{n\to\infty} \mathbb{E}[r_n] = 0.$$

*Proof.* See Appendix L □

Intuitively, this theorem states that as the action space become more dense and complex, the actions sampled for search become increasingly less diverse, which strongly impedes successful planning. Note that this analysis is strictly more general than the last experiment, where we simply copied the available actions. Further analysis of the experiments involving large action spaces is provided in Appendix B.3.

**Takeaway** *When facing a problem with a complex action space, subgoal methods should outperform low-level search (Q2).*

### 5.4 Subgoal Methods Avoid Dead Ends

Once an agent encounters a dead end, reaching the goal becomes impossible, leading to wasted computational effort. Our results, presented in Figure 5.4, show that subgoal methods tend to enter dead ends less often than low-level methods. Using longer subgoals improves the ability to bypass those areas.

Among low-level methods, $\rho$-A* performs the best at minimizing dead ends rate, as its node selection regularizes values by depth in the search tree, preventing it from over-committing to dead ends. However, even $\rho$-A* is outperformed by subgoal methods, which rely on greedy value estimates and subgoals.

Deciding whether a state is a dead end can be NP-hard. Hence, it is much harder for the value function to penalize dead ends compared to the policy, which only ranks the available actions and does not have to identify dead ends (Feng et al., 2022). Furthermore, demonstrations used for imitation learning lead to the goal state, hence they contain no dead ends. Therefore the value function trained this way is never directly instructed to penalize dead ends. At the same time, during training of the policy the actions leading to dead ends are never reinforced. Our experiments show that hierarchical search relies much less on the value guidance compared to low-level search (Section 5.2), which further supports our conclusions. For a more detailed analysis, see Appendix B.4.

| Search algorithm | Dead ends rate |
|---|---|
| $\rho$-MCTS | 22.0% |
| $\rho$-BestFS | 18.5% |
| $\rho$-A* | 13.7% |
| kSubS (4 steps) | 12.7% |
| kSubS (8 steps) | 10.0% |
| AdaSubS | 8.86% |

Figure 12: Fraction of dead ends encountered during search between hierarchical and low-level methods in Sokoban.

**Takeaway** *Subgoal Methods Are More Effective at Avoiding Dead Ends Compared to Low-Level Search (Q2).*

### 5.5 Subgoal Methods Generalize Out-Of-Distribution

Planners that can generalize to out-of-distribution (OOD) instances are essential for robust decision-making (Kirk et al., 2023; Shen et al., 2021). We tested two types of generalization in the Sokoban environment: by significantly changing the layout of the board and by using extremely difficult boards from the DeepMind dataset (Guez et al., 2018) (see Figure 13 for examples).

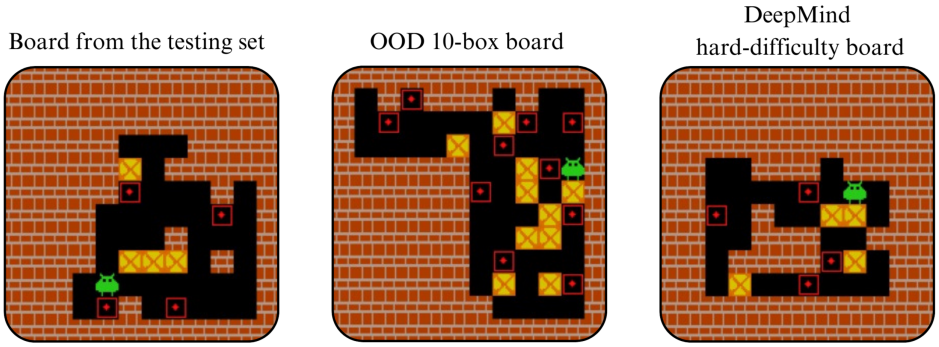


Figure 13: Examples of Sokoban boards used in OOD experiments

In both cases, subgoal methods show better performance than low-level methods, with the gap increasing as the distribution shift become more visible (see Figures 14-15). However, we found that kSubS, when using twice longer subgoals, collapses in OOD evaluations, despite outperforming $\rho$-BestFS and other low-level methods on in-distribution tasks. As the subgoal distance increases, predicting the distant future becomes more challenging, making it less likely for the generated subgoals to be valid and reachable, especially in OOD tasks. In contrast, low-level methods avoid this issue, as selecting an action from a limited set always

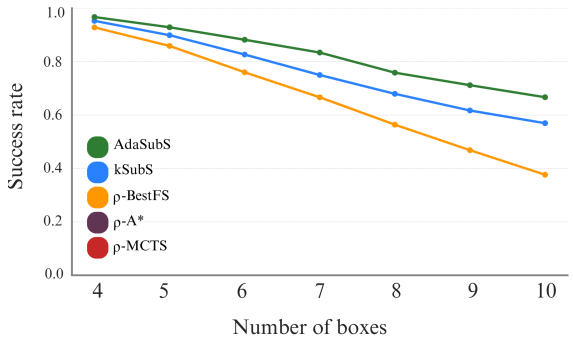


Figure 14: Averaged OOD results on Sokoban boards with OOD layouts. These instances were generated by systematically varying all parameters of the instance generator.

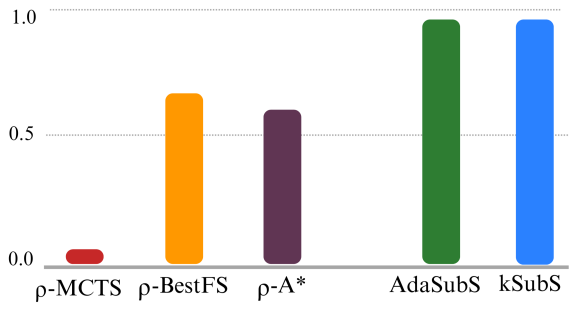


Figure 15: Performance on DeepMind extra hard boards.

results in a valid move. Thus, while subgoal methods can be effective in OOD scenarios, excessively long subgoals can degrade performance (Q2).

When evaluated on extremely challenging instances (see Figure 1) introduced by (Guez et al., 2018), all methods required a significantly higher search budget but maintained the same performance order as in the previous experiment (Q1). Solving these instances requires more advanced strategies than those learned during training. Subgoal methods are better equipped to handle this increased complexity because selecting subgoals is closely related to choosing a broader strategy because of their longer horizon. In contrast, low-level methods must assess each individual action, which limits their ability to foresee the long-term consequences of their choices.

**Takeaway** *Subgoal methods can scale better than low-level methods on OOD instances, provided the subgoals are not too long (Q2).*

## 6 Discussion of the Results and Future Directions

While we identified several features that facilitate the performance of subgoal methods, that list is not exhaustive. As our study is mostly empirical, it is hard to strongly support truly universal claims this way. Thus, it is essential to study this topic further, expand the analysis to more subgoal-based and low-level algorithms, and include even more types of environments. While most of our takeaways were confirmed in multiple environments, extending the evaluation to more domains would strengthen our conclusions.

While empirical results suggest general trends, Theorems 1-2 provide theoretical support for key findings. These theorems apply to the general class of hierarchical methods as described in Section 4, reinforcing their broader relevance. We believe that other results can serve as a direction for further theoretical study as well.

Our study has broader implications for other complex domains. For example, advancements in robotics often face significant challenges due to limited data, leading many methods to rely on collective datasets like Open X-Embodiment (Collaboration et al., 2023). As shown in our experiments, hierarchical search methods benefit substantially from training on diverse expert data (Section 5.1). Furthermore, the data bottleneck increases the need for the models to generalize to out-of-distribution scenes and tasks, which is also an advantage of hierarchical methods (Section 5.5). Finally, an essential aspect of robotics involves preventing the robot from becoming stuck or losing the manipulated object, events that can be seen as dead-end scenarios (Section 5.4). Successful applications of hierarchical methods in robotics include models such as SuSIE (Black et al., 2024) and HIQL (Park et al., 2023).

Additionally, our experiments indicate that hierarchical methods scale well in long-horizon tasks, as evidenced by their performance in the N-Puzzle and the Rubik's Cube (using Beginner demonstrations), where the average sequence of steps often exceeds 200. Interestingly, while low-level methods can still perform well in these scenarios, we observed that they tend to be much more sensitive to hyperparameter tuning.

It is important to note that we do not claim hierarchical methods are universally superior to low-level approaches in all complex domains. Instead, the properties highlighted in our analysis suggest cases where they should be considered.

## 7 Conclusions

We conducted a thorough comparison of hierarchical and low-level search methods for combinatorial tasks. Our experiments provides empirical and some theoretical evidence that hierarchical approaches should be preferred in environments where value estimation is challenging and learned estimates face significant uncertainty, particularly when learning from diverse suboptimal data. Furthermore, subgoal methods demonstrate better scalability in complex action spaces and are more effective at avoiding dead ends than low-level methods. Thus, in environments characterized by those properties, it is advisable to consider subgoal methods as an alternative to low-level search.

Based on our results, we propose guidelines for future research in this area. According to our experiments, the best-performing low-level search was usually $\rho$-BestFS with a confidence threshold (see Appendix F). Although it is rather sensitive to the threshold value, which has to be optimized for each domain separately, we advocate using this simple method as a standard baseline for further research in hierarchical search. Our guidelines are comprehensively discussed in Appendix J.

Additionally, we identified easy-to-overlook mistakes in reporting the results that may lead to misleading conclusions. Most importantly, the reported *complete search budget* of hierarchical methods must include all the visited states and not only the high-level nodes as used in some prior works.

## 8 Reproducibility Statement

The code used to run all our experiments is available at `https://github.com/subgoalsearchmatters/what-matters-in-hierarchical-search`. We also link there datasets used for training our models. Hence, all our results are fully reproducible.

## References

Joshua Achiam, David Held, Aviv Tamar, and Pieter Abbeel. Constrained policy optimization. In Doina Precup and Yee Whye Teh (eds.), *Proceedings of the 34th International Conference on Machine Learning, ICML 2017, Sydney, NSW, Australia, 6-11 August 2017*, volume 70 of *Proceedings of Machine Learning Research*, pp. 22–31. PMLR, 2017. URL `http://proceedings.mlr.press/v70/achiam17a.html`.

Marcin Andrychowicz, Anton Raichuk, Piotr Stanczyk, Manu Orsini, Sertan Girgin, Raphaël Marinier, Léonard Hussenot, Matthieu Geist, Olivier Pietquin, Marcin Michalski, Sylvain Gelly, and Olivier Bachem. What matters in on-policy reinforcement learning? A large-scale empirical study. *CoRR*, abs/2006.05990, 2020. URL `https://arxiv.org/abs/2006.05990`.

David L Applegate, Robert E Bixby, Václav Chvátal, and William J Cook. *The Traveling Salesman Problem: A Computational Study*. Princeton University Press, 2006.

Chris L Baker, Rebecca Saxe, and Joshua B Tenenbaum. Action understanding as inverse planning. *Cognition*, 113(3):329–349, 2009.

Yoshua Bengio, Andrea Lodi, and Antoine Prouvost. Learning combinatorial optimization algorithms over graphs. In *Advances in Neural Information Processing Systems*, 2021.

Kevin Black, Mitsuhiko Nakamoto, Pranav Atreya, Homer Rich Walke, Chelsea Finn, Aviral Kumar, and Sergey Levine. Zero-shot robotic manipulation with pre-trained image-editing diffusion models. In *The Twelfth International Conference on Learning Representations, ICLR 2024, Vienna, Austria, May 7-11, 2024*. OpenReview.net, 2024. URL https://openreview.net/forum?id=c0chJTSbci.

Jehoshua Bruck and Joseph W. Goodman. On the power of neural networks for solving hard problems. In Dana Z. Anderson (ed.), *Neural Information Processing Systems, Denver, Colorado, USA, 1987*, pp. 137–143. American Institue of Physics, 1987. URL http://papers.nips.cc/paper/70-on-the-power-of-neural-networks-for-solving-hard-problems.

Robert Brunetto and Otakar Trunda. Deep heuristic-learning in the rubik's cube domain: An experimental evaluation. In Jaroslava Hlavácová (ed.), *Proceedings of the 17th Conference on Information Technologies - Applications and Theory (ITAT 2017), Martinské hole, Slovakia, September 22-26, 2017*, volume 1885 of *CEUR Workshop Proceedings*, pp. 57–64. CEUR-WS.org, 2017. URL https://ceur-ws.org/Vol-1885/57.pdf.

Murray Campbell, A. Joseph Hoane Jr., and Feng-Hsiung Hsu. Deep blue. *Artif. Intell.*, 134(1-2):57–83, 2002. doi: 10.1016/S0004-3702(01)00129-1. URL https://doi.org/10.1016/S0004-3702(01)00129-1.

Chang Chen, Fei Deng, Kenji Kawaguchi, Çaglar Gülçehre, and Sungjin Ahn. Simple hierarchical planning with diffusion. *CoRR*, abs/2401.02644, 2024. doi: 10.48550/ARXIV.2401.02644. URL https://doi.org/10.48550/arXiv.2401.02644.

Lili Chen, Kevin Lu, Aravind Rajeswaran, Kimin Lee, Aditya Grover, Michael Laskin, Pieter Abbeel, Aravind Srinivas, and Igor Mordatch. Decision transformer: Reinforcement learning via sequence modeling. In Marc'Aurelio Ranzato, Alina Beygelzimer, Yann N. Dauphin, Percy Liang, and Jennifer Wortman Vaughan (eds.), *Advances in Neural Information Processing Systems 34: Annual Conference on Neural Information Processing Systems 2021, NeurIPS 2021, December 6-14, 2021, virtual*, pp. 15084–15097, 2021. URL https://proceedings.neurips.cc/paper/2021/hash/7f489f642a0ddb10272b5c31057f0663-Abstract.html.

Howie Choset, Kevin M. Lynch, Seth Hutchinson, George Kantor, Wolfram Burgard, Lydia E. Kavraki, and Sebastian Thrun. *Principles of Robot Motion: Theory, Algorithms, and Implementations*. MIT Press, Cambridge, MA, 2005. ISBN 978-0-262-03327-5.

Open X-Embodiment Collaboration, Abby O'Neill, Abdul Rehman, Abhiram Maddukuri, Abhishek Gupta, Abhishek Padalkar, Abraham Lee, Acorn Pooley, Agrim Gupta, Ajay Mandlekar, Ajinkya Jain, Albert Tung, Alex Bewley, Alex Herzog, Alex Irpan, Alexander Khazatsky, Anant Rai, Anchit Gupta, Andrew Wang, Anikait Singh, Animesh Garg, Aniruddha Kembhavi, Annie Xie, Anthony Brohan, Antonin Raffin, Archit Sharma, Arefeh Yavary, Arhan Jain, Ashwin Balakrishna, Ayzaan Wahid, Ben Burgess-Limerick, Beomjoon Kim, Bernhard Schölkopf, Blake Wulfe, Brian Ichter, Cewu Lu, Charles Xu, Charlotte Le, Chelsea Finn, Chen Wang, Chenfeng Xu, Cheng Chi, Chenguang Huang, Christine Chan, Christopher Agia, Chuer Pan, Chuyuan Fu, Coline Devin, Danfei Xu, Daniel Morton, Danny Driess, Daphne Chen, Deepak Pathak, Dhruv Shah, Dieter Büchler, Dinesh Jayaraman, Dmitry Kalashnikov, Dorsa Sadigh, Edward Johns, Ethan Foster, Fangchen Liu, Federico Ceola, Fei Xia, Feiyu Zhao, Freek Stulp, Gaoyue Zhou, Gaurav S. Sukhatme, Gautam Salhotra, Ge Yan, Gilbert Feng, Giulio Schiavi, Glen Berseth, Gregory Kahn, Guanzhi Wang, Hao Su, Hao-Shu Fang, Haochen Shi, Henghui Bao, Heni Ben Amor, Henrik I Christensen, Hiroki Furuta, Homer Walke, Hongjie Fang, Huy Ha, Igor Mordatch, Ilija Radosavovic, Isabel Leal, Jacky Liang, Jad Abou-Chakra, Jaehyung Kim, Jaimyn Drake, Jan Peters, Jan Schneider, Jasmine Hsu, Jeannette Bohg, Jeffrey Bingham, Jeffrey Wu, Jensen Gao, Jiaheng Hu, Jiajun Wu, Jialin Wu, Jiankai Sun, Jianlan Luo, Jiayuan Gu, Jie Tan, Jihoon Oh, Jimmy Wu, Jingpei Lu, Jingyun Yang, Jitendra Malik, João Silvério, Joey Hejna, Jonathan Booher, Jonathan Tompson, Jonathan Yang, Jordi Salvador, Joseph J. Lim, Junhyek Han, Kaiyuan Wang, Kanishka Rao, Karl Pertsch, Karol Hausman, Keegan Go, Keerthana Gopalakrishnan, Ken Goldberg, Kendra Byrne, Kenneth Oslund, Kento Kawaharazuka, Kevin Black, Kevin Lin, Kevin Zhang, Kiana Ehsani, Kiran Lekkala, Kirsty Ellis, Krishan Rana, Krishnan Srinivasan, Kuan Fang, Kunal Pratap Singh, Kuo-Hao Zeng, Kyle Hatch, Kyle Hsu, Laurent Itti, Lawrence Yunliang Chen, Lerrel Pinto, Li Fei-Fei, Liam Tan, Linxi "Jim" Fan, Lionel Ott, Lisa Lee, Luca

Weihs, Magnum Chen, Marion Lepert, Marius Memmel, Masayoshi Tomizuka, Masha Itkina, Mateo Guaman Castro, Max Spero, Maximilian Du, Michael Ahn, Michael C. Yip, Mingtong Zhang, Mingyu Ding, Minho Heo, Mohan Kumar Srirama, Mohit Sharma, Moo Jin Kim, Naoaki Kanazawa, Nicklas Hansen, Nicolas Heess, Nikhil J Joshi, Niko Suenderhauf, Ning Liu, Norman Di Palo, Nur Muhammad Mahi Shafiullah, Oier Mees, Oliver Kroemer, Osbert Bastani, Pannag R Sanketi, Patrick "Tree" Miller, Patrick Yin, Paul Wohlhart, Peng Xu, Peter David Fagan, Peter Mitrano, Pierre Sermanet, Pieter Abbeel, Priya Sundaresan, Qiuyu Chen, Quan Vuong, Rafael Rafailov, Ran Tian, Ria Doshi, Roberto Mart'in-Mart'in, Rohan Baijal, Rosario Scalise, Rose Hendrix, Roy Lin, Runjia Qian, Ruohan Zhang, Russell Mendonca, Rutav Shah, Ryan Hoque, Ryan Julian, Samuel Bustamante, Sean Kirmani, Sergey Levine, Shan Lin, Sherry Moore, Shikhar Bahl, Shivin Dass, Shubham Sonawani, Shuran Song, Sichun Xu, Siddhant Haldar, Siddharth Karamcheti, Simeon Adebola, Simon Guist, Soroush Nasiriany, Stefan Schaal, Stefan Welker, Stephen Tian, Subramanian Ramamoorthy, Sudeep Dasari, Suneel Belkhale, Sungjae Park, Suraj Nair, Suvir Mirchandani, Takayuki Osa, Tanmay Gupta, Tatsuya Harada, Tatsuya Matsushima, Ted Xiao, Thomas Kollar, Tianhe Yu, Tianli Ding, Todor Davchev, Tony Z. Zhao, Travis Armstrong, Trevor Darrell, Trinity Chung, Vidhi Jain, Vincent Vanhoucke, Wei Zhan, Wenxuan Zhou, Wolfram Burgard, Xi Chen, Xiaolong Wang, Xinghao Zhu, Xinyang Geng, Xiyuan Liu, Xu Liangwei, Xuanlin Li, Yao Lu, Yecheng Jason Ma, Yejin Kim, Yevgen Chebotar, Yifan Zhou, Yifeng Zhu, Yilin Wu, Ying Xu, Yixuan Wang, Yonatan Bisk, Yoonyoung Cho, Youngwoon Lee, Yuchen Cui, Yue Cao, Yueh-Hua Wu, Yujin Tang, Yuke Zhu, Yunchu Zhang, Yunfan Jiang, Yunshuang Li, Yunzhu Li, Yusuke Iwasawa, Yutaka Matsuo, Zehan Ma, Zhuo Xu, Zichen Jeff Cui, Zichen Zhang, and Zipeng Lin. Open X-Embodiment: Robotic learning datasets and RT-X models. https://arxiv.org/abs/2310.08864, 2023.

Thomas H. Cormen, Charles E. Leiserson, Ronald L. Rivest, and Clifford Stein. *Introduction to Algorithms, Third Edition*. The MIT Press, 3rd edition, 2009. ISBN 0262033844.

Joseph C. Culberson. Sokoban is pspace-complete. 1997. URL https://api.semanticscholar.org/CorpusID:61114368.

Konrad Czechowski, Tomasz Odrzygózdz, Marek Zbysinski, Michal Zawalski, Krzysztof Olejnik, Yuhuai Wu, Lukasz Kucinski, and Piotr Milos. Subgoal search for complex reasoning tasks. In Marc'Aurelio Ranzato, Alina Beygelzimer, Yann N. Dauphin, Percy Liang, and Jennifer Wortman Vaughan (eds.), *Advances in Neural Information Processing Systems 34: Annual Conference on Neural Information Processing Systems 2021, NeurIPS 2021, December 6-14, 2021, virtual*, pp. 624–638, 2021. URL https://proceedings.neurips.cc/paper/2021/hash/05d8cccb5f47e5072f0a05b5f514941a-Abstract.html.

Erik D. Demaine, Sarah Eisenstat, and Mikhail Rudoy. Solving the rubik's cube optimally is np-complete. Schloss Dagstuhl – Leibniz-Zentrum für Informatik, 2018. doi: 10.4230/LIPICS.STACS.2018.24. URL https://drops.dagstuhl.de/entities/document/10.4230/LIPIcs.STACS.2018.24.

Jacob Devlin, Ming-Wei Chang, Kenton Lee, and Kristina Toutanova. BERT: Pre-training of deep bidirectional transformers for language understanding. In Jill Burstein, Christy Doran, and Thamar Solorio (eds.), *Proceedings of the 2019 Conference of the North American Chapter of the Association for Computational Linguistics: Human Language Technologies, Volume 1 (Long and Short Papers)*, pp. 4171–4186, Minneapolis, Minnesota, June 2019. Association for Computational Linguistics. doi: 10.18653/v1/N19-1423. URL https://aclanthology.org/N19-1423.

Alexey Dosovitskiy, German Ros, Felipe Codevilla, Antonio Lopez, and Vladlen Koltun. CARLA: An open urban driving simulator. In *Proceedings of the 1st Annual Conference on Robot Learning*, pp. 1–16, 2017.

Gabriel Dulac-Arnold, Richard Evans, Peter Sunehag, and Ben Coppin. Reinforcement learning in large discrete action spaces. *CoRR*, abs/1512.07679, 2015. URL http://arxiv.org/abs/1512.07679.

Mark Edmonds, Feng Gao, Xu Xie, Hangxin Liu, Siyuan Qi, Yixin Zhu, Brandon Rothrock, and Song-Chun Zhu. Feeling the force: Integrating force and pose for fluent discovery through imitation learning to open medicine bottles. In *2017 IEEE/RSJ International Conference on Intelligent Robots and Systems (IROS)*, pp. 3530–3537, 2017. doi: 10.1109/IROS.2017.8206196.

Ben Eysenbach, Russ R Salakhutdinov, and Sergey Levine. Search on the replay buffer: Bridging planning and reinforcement learning. In H. Wallach, H. Larochelle, A. Beygelzimer, F. d'Alché-Buc, E. Fox, and R. Garnett (eds.), *Advances in Neural Information Processing Systems*, volume 32. Curran Associates, Inc., 2019. URL https://proceedings.neurips.cc/paper_files/paper/2019/file/5c48ff18e0a47baaf81d8b8ea51eec92-Paper.pdf.

Mehdi Fatemi, Taylor W. Killian, Jayakumar Subramanian, and Marzyeh Ghassemi. Medical dead-ends and learning to identify high-risk states and treatments. In Marc'Aurelio Ranzato, Alina Beygelzimer, Yann N. Dauphin, Percy Liang, and Jennifer Wortman Vaughan (eds.), *Advances in Neural Information Processing Systems 34: Annual Conference on Neural Information Processing Systems 2021, NeurIPS 2021, December 6-14, 2021, virtual*, pp. 4856–4870, 2021. URL https://proceedings.neurips.cc/paper/2021/hash/26405399c51ad7b13b504e74eb7c696c-Abstract.html.

Dieqiao Feng, Carla P Gomes, and Bart Selman. Left heavy tails and the effectiveness of the policy and value networks in DNN-based best-first search for sokoban planning. In Alice H. Oh, Alekh Agarwal, Danielle Belgrave, and Kyunghyun Cho (eds.), *Advances in Neural Information Processing Systems*, 2022. URL https://openreview.net/forum?id=b6to5kfFhQh.

Arnaud Fickinger, Samuel Cohen, Stuart Russell, and Brandon Amos. Cross-domain imitation learning via optimal transport. In *International Conference on Learning Representations*, 2022. URL https://openreview.net/forum?id=xP3cPq2hQC.

Ayelet Fishbach and Ravi Dhar. Goals as excuses or guides: The liberating effect of perceived goal progress on choice. *Journal of Consumer Research*, 32(3):370–377, 2005.

Justin Fu, Aviral Kumar, Ofir Nachum, George Tucker, and Sergey Levine. D4RL: datasets for deep data-driven reinforcement learning. *CoRR*, abs/2004.07219, 2020. URL https://arxiv.org/abs/2004.07219.

Mohammad Ghavamzadeh and Sridhar Mahadevan. Hierarchical policy gradient algorithms. In Tom Fawcett and Nina Mishra (eds.), *Machine Learning, Proceedings of the Twentieth International Conference (ICML 2003), August 21-24, 2003, Washington, DC, USA*, pp. 226–233. AAAI Press, 2003. URL http://www.aaai.org/Library/ICML/2003/icml03-032.php.

Kristen Grauman, Andrew Westbury, Eugene Byrne, Zachary Chavis, Antonino Furnari, Rohit Girdhar, Jackson Hamburger, Hao Jiang, Miao Liu, Xingyu Liu, Miguel Martin, Tushar Nagarajan, Ilija Radosavovic, Santhosh Kumar Ramakrishnan, Fiona Ryan, Jayant Sharma, Michael Wray, Mengmeng Xu, Eric Zhongcong Xu, Chen Zhao, Siddhant Bansal, Dhruv Batra, Vincent Cartillier, Sean Crane, Tien Do, Morrie Doulaty, Akshay Erapalli, Christoph Feichtenhofer, Adriano Fragomeni, Qichen Fu, Abrham Gebreselasie, Cristina Gonzalez, James Hillis, Xuhua Huang, Yifei Huang, Wenqi Jia, Weslie Khoo, Jachym Kolar, Satwik Kottur, Anurag Kumar, Federico Landini, Chao Li, Yanghao Li, Zhenqiang Li, Karttikeya Mangalam, Raghava Modhugu, Jonathan Munro, Tullie Murrell, Takumi Nishiyasu, Will Price, Paola Ruiz Puentes, Merey Ramazanova, Leda Sari, Kiran Somasundaram, Audrey Southerland, Yusuke Sugano, Ruijie Tao, Minh Vo, Yuchen Wang, Xindi Wu, Takuma Yagi, Ziwei Zhao, Yunyi Zhu, Pablo Arbelaez, David Crandall, Dima Damen, Giovanni Maria Farinella, Christian Fuegen, Bernard Ghanem, Vamsi Krishna Ithapu, C. V. Jawahar, Hanbyul Joo, Kris Kitani, Haizhou Li, Richard Newcombe, Aude Oliva, Hyun Soo Park, James M. Rehg, Yoichi Sato, Jianbo Shi, Mike Zheng Shou, Antonio Torralba, Lorenzo Torresani, Mingfei Yan, and Jitendra Malik. Ego4d: Around the world in 3,000 hours of egocentric video, 2022.

Arthur Guez, Mehdi Mirza, Karol Gregor, Rishabh Kabra, Sebastien Racaniere, Theophane Weber, David Raposo, Adam Santoro, Laurent Orseau, Tom Eccles, Greg Wayne, David Silver, Timothy Lillicrap, and Victor Valdes. An investigation of model-free planning: boxoban levels. https://github.com/deepmind/boxoban-levels/, 2018.

Patrik Haslum, Nir Lipovetzky, Daniele Magazzeni, and Christian Muise. *An Introduction to the Planning Domain Definition Language*. Synthesis Lectures on Artificial Intelligence and Machine Learning. Morgan & Claypool Publishers, 2019. ISBN 978-3-031-00456-8. doi: 10.2200/S00900ED2V01Y201902AIM042. URL https://doi.org/10.2200/S00900ED2V01Y201902AIM042.

Zhiao Huang, Fangchen Liu, and Hao Su. Mapping state space using landmarks for universal goal reaching. In Hanna M. Wallach, Hugo Larochelle, Alina Beygelzimer, Florence d'Alché-Buc, Emily B. Fox, and Roman Garnett (eds.), *Advances in Neural Information Processing Systems 32: Annual Conference on Neural Information Processing Systems 2019, NeurIPS 2019, December 8-14, 2019, Vancouver, BC, Canada*, pp. 1940–1950, 2019. URL https://proceedings.neurips.cc/paper/2019/hash/3b712de48137572f3849aabd5666a4e3-Abstract.html.

Clark L. Hull. The goal gradient hypothesis and maze learning. *Psychological Review*, 39(1):25–43, 1932.

Steven James, George Konidaris, and Benjamin Rosman. An analysis of monte carlo tree search. *Proceedings of the AAAI Conference on Artificial Intelligence*, 31(1), Feb. 2017. doi: 10.1609/aaai.v31i1.11028. URL https://ojs.aaai.org/index.php/AAAI/article/view/11028.

Yiding Jiang, Shixiang Gu, Kevin Murphy, and Chelsea Finn. Language as an abstraction for hierarchical deep reinforcement learning. In Hanna M. Wallach, Hugo Larochelle, Alina Beygelzimer, Florence d'Alché-Buc, Emily B. Fox, and Roman Garnett (eds.), *Advances in Neural Information Processing Systems 32: Annual Conference on Neural Information Processing Systems 2019, NeurIPS 2019, December 8-14, 2019, Vancouver, BC, Canada*, pp. 9414–9426, 2019. URL https://proceedings.neurips.cc/paper/2019/hash/0af787945872196b42c9f73ead2565c8-Abstract.html.

Michael Kelly, Chelsea Sidrane, Katherine Driggs-Campbell, and Mykel J. Kochenderfer. Hg-dagger: Interactive imitation learning with human experts. In *2019 International Conference on Robotics and Automation (ICRA)*, pp. 8077–8083, 2019. doi: 10.1109/ICRA.2019.8793698.

Kuno Kim, Yihong Gu, Jiaming Song, Shengjia Zhao, and Stefano Ermon. Domain adaptive imitation learning. In Hal Daumé III and Aarti Singh (eds.), *Proceedings of the 37th International Conference on Machine Learning*, volume 119 of *Proceedings of Machine Learning Research*, pp. 5286–5295. PMLR, 13–18 Jul 2020. URL https://proceedings.mlr.press/v119/kim20c.html.

Moo Jin Kim, Karl Pertsch, Siddharth Karamcheti, Ted Xiao, Ashwin Balakrishna, Suraj Nair, Rafael Rafailov, Ethan Foster, Grace Lam, Pannag Sanketi, Quan Vuong, Thomas Kollar, Benjamin Burchfiel, Russ Tedrake, Dorsa Sadigh, Sergey Levine, Percy Liang, and Chelsea Finn. Openvla: An open-source vision-language-action model. *arXiv preprint arXiv:2406.09246*, 2024.

Thomas N. Kipf and Max Welling. Semi-supervised classification with graph convolutional networks. In *5th International Conference on Learning Representations, ICLR 2017, Toulon, France, April 24-26, 2017, Conference Track Proceedings*. OpenReview.net, 2017. URL https://openreview.net/forum?id=SJU4ayYgl.

B. Ravi Kiran, Ibrahim Sobh, Victor Talpaert, Patrick Mannion, Ahmad A. Al Sallab, Senthil Kumar Yogamani, and Patrick Pérez. Deep reinforcement learning for autonomous driving: A survey. *IEEE Trans. Intell. Transp. Syst.*, 23(6):4909–4926, 2022. doi: 10.1109/TITS.2021.3054625. URL https://doi.org/10.1109/TITS.2021.3054625.

Robert Kirk, Amy Zhang, Edward Grefenstette, and Tim Rocktäschel. A survey of zero-shot generalisation in deep reinforcement learning. *J. Artif. Intell. Res.*, 76:201–264, 2023. doi: 10.1613/JAIR.1.14174. URL https://doi.org/10.1613/jair.1.14174.

Wouter Kool and Matthew Botvinick. A labor/leisure tradeoff in cognitive control. *Journal of Experimental Psychology: General*, 143(1):131–141, 2014.

Kalle Kujanpää, Joni Pajarinen, and Alexander Ilin. Hierarchical imitation learning with vector quantized models. In Andreas Krause, Emma Brunskill, Kyunghyun Cho, Barbara Engelhardt, Sivan Sabato, and Jonathan Scarlett (eds.), *International Conference on Machine Learning, ICML 2023, 23-29 July 2023, Honolulu, Hawaii, USA*, volume 202 of *Proceedings of Machine Learning Research*, pp. 17896–17919. PMLR, 2023a. URL https://proceedings.mlr.press/v202/kujanpaa23a.html.

Kalle Kujanpää, Joni Pajarinen, and Alexander Ilin. Hybrid search for efficient planning with completeness guarantees. *CoRR*, abs/2310.12819, 2023b. doi: 10.48550/ARXIV.2310.12819. URL https://doi.org/10.48550/arXiv.2310.12819.

Aviral Kumar, Joey Hong, Anikait Singh, and Sergey Levine. When should we prefer offline reinforcement learning over behavioral cloning? *CoRR*, abs/2204.05618, 2022. doi: 10.48550/ARXIV.2204.05618. URL https://doi.org/10.48550/arXiv.2204.05618.

Steven M LaValle. *Planning algorithms*. Cambridge university press, 2006.

Seungjae Lee, Jigang Kim, Inkyu Jang, and H. Jin Kim. DHRL: A graph-based approach for long-horizon and sparse hierarchical reinforcement learning. In Sanmi Koyejo, S. Mohamed, A. Agarwal, Danielle Belgrave, K. Cho, and A. Oh (eds.), *Advances in Neural Information Processing Systems 35: Annual Conference on Neural Information Processing Systems 2022, NeurIPS 2022, New Orleans, LA, USA, November 28 - December 9, 2022*, 2022. URL http://papers.nips.cc/paper_files/paper/2022/hash/58b286aea34a91a3d33e58af0586fa40-Abstract-Conference.html.

Sergey Levine, Aviral Kumar, George Tucker, and Justin Fu. Offline reinforcement learning: Tutorial, review, and perspectives on open problems. *CoRR*, abs/2005.01643, 2020. URL https://arxiv.org/abs/2005.01643.

Andrew Levy, George Dimitri Konidaris, Robert Platt Jr., and Kate Saenko. Learning multi-level hierarchies with hindsight. In *7th International Conference on Learning Representations, ICLR 2019, New Orleans, LA, USA, May 6-9, 2019*. OpenReview.net, 2019. URL https://openreview.net/forum?id=ryzECoAcY7.

Mike Lewis, Yinhan Liu, Naman Goyal, Marjan Ghazvininejad, Abdelrahman Mohamed, Omer Levy, Veselin Stoyanov, and Luke Zettlemoyer. BART: Denoising sequence-to-sequence pre-training for natural language generation, translation, and comprehension. In Dan Jurafsky, Joyce Chai, Natalie Schluter, and Joel Tetreault (eds.), *Proceedings of the 58th Annual Meeting of the Association for Computational Linguistics*, pp. 7871–7880, Online, July 2020. Association for Computational Linguistics. doi: 10.18653/v1/2020.acl-main.703. URL https://aclanthology.org/2020.acl-main.703.

Quanyi Li, Zhenghao Peng, and Bolei Zhou. Efficient learning of safe driving policy via human-ai copilot optimization. In *International Conference on Learning Representations*, 2022. URL https://openreview.net/forum?id=0cgU-BZp2ky.

Ajay Mandlekar, Yuke Zhu, Animesh Garg, Jonathan Booher, Max Spero, Albert Tung, Julian Gao, John Emmons, Anchit Gupta, Emre Orbay, Silvio Savarese, and Li Fei-Fei. ROBOTURK: A crowdsourcing platform for robotic skill learning through imitation. In *2nd Annual Conference on Robot Learning, CoRL 2018, Zürich, Switzerland, 29-31 October 2018, Proceedings*, volume 87 of *Proceedings of Machine Learning Research*, pp. 879–893. PMLR, 2018. URL http://proceedings.mlr.press/v87/mandlekar18a.html.

Stephen McAleer, Forest Agostinelli, Alexander Shmakov, and Pierre Baldi. Solving the rubik's cube with approximate policy iteration. In *7th International Conference on Learning Representations, ICLR 2019, New Orleans, LA, USA, May 6-9, 2019*. OpenReview.net, 2019. URL https://openreview.net/forum?id=Hyfn2jCcKm.

Oier Mees, Lukás Hermann, and Wolfram Burgard. What matters in language conditioned robotic imitation learning over unstructured data. *IEEE Robotics Autom. Lett.*, 7(4):11205–11212, 2022. doi: 10.1109/LRA.2022.3196123. URL https://doi.org/10.1109/LRA.2022.3196123.

Volodymyr Mnih, Koray Kavukcuoglu, David Silver, Andrei A Rusu, Joel Veness, Marc G Bellemare, Alex Graves, Martin Riedmiller, Andreas K Fidjeland, Georg Ostrovski, Stig Petersen, et al. Human-level control through deep reinforcement learning. *Nature*, 518(7540):529–533, 2015.

Ofir Nachum, Shixiang Gu, Honglak Lee, and Sergey Levine. Data-efficient hierarchical reinforcement learning. In Samy Bengio, Hanna M. Wallach, Hugo Larochelle, Kristen Grauman, Nicolò Cesa-Bianchi, and Roman Garnett (eds.), *Advances in Neural Information Processing Systems 31: Annual Conference on Neural Information Processing Systems 2018, NeurIPS 2018, December 3-8, 2018, Montréal, Canada*, pp. 3307–3317, 2018. URL https://proceedings.neurips.cc/paper/2018/hash/e6384711491713d29bc63fc5eeb5ba4f-Abstract.html.

Ashvin Nair, Bob McGrew, Marcin Andrychowicz, Wojciech Zaremba, and Pieter Abbeel. Overcoming exploration in reinforcement learning with demonstrations. In *2018 IEEE International Conference on Robotics and Automation, ICRA 2018, Brisbane, Australia, May 21-25, 2018*, pp. 6292–6299. IEEE, 2018. doi: 10.1109/ICRA.2018.8463162. URL https://doi.org/10.1109/ICRA.2018.8463162.

Saul B Needleman and Christian D Wunsch. A general method applicable to the search for similarities in the amino acid sequence of two proteins. *Journal of molecular biology*, 48(3):443–453, 1970.

Laurent Orseau and Levi H. S. Lelis. Policy-guided heuristic search with guarantees. In *Thirty-Fifth AAAI Conference on Artificial Intelligence, AAAI 2021, Thirty-Third Conference on Innovative Applications of Artificial Intelligence, IAAI 2021, The Eleventh Symposium on Educational Advances in Artificial Intelligence, EAAI 2021, Virtual Event, February 2-9, 2021*, pp. 12382–12390. AAAI Press, 2021. doi: 10.1609/AAAI.V35I14.17469. URL https://doi.org/10.1609/aaai.v35i14.17469.

Laurent Orseau, Marcus Hutter, and Levi H. S. Lelis. Levin tree search with context models. In Edith Elkind (ed.), *Proceedings of the Thirty-Second International Joint Conference on Artificial Intelligence, IJCAI-23*, pp. 5622–5630. International Joint Conferences on Artificial Intelligence Organization, 8 2023. doi: 10.24963/ijcai.2023/624. URL https://doi.org/10.24963/ijcai.2023/624. Main Track.

Aleksandr I. Panov and Aleksey Skrynnik. Automatic formation of the structure of abstract machines in hierarchical reinforcement learning with state clustering. *CoRR*, abs/1806.05292, 2018. URL http://arxiv.org/abs/1806.05292.

Seohong Park, Dibya Ghosh, Benjamin Eysenbach, and Sergey Levine. HIQL: offline goal-conditioned RL with latent states as actions. In Alice Oh, Tristan Naumann, Amir Globerson, Kate Saenko, Moritz Hardt, and Sergey Levine (eds.), *Advances in Neural Information Processing Systems 36: Annual Conference on Neural Information Processing Systems 2023, NeurIPS 2023, New Orleans, LA, USA, December 10 - 16, 2023*, 2023. URL http://papers.nips.cc/paper_files/paper/2023/hash/6d7c4a0727e089ed6cdd3151cbe8d8ba-Abstract-Conference.html.

Karl Pertsch, Oleh Rybkin, Frederik Ebert, Shenghao Zhou, Dinesh Jayaraman, Chelsea Finn, and Sergey Levine. Long-horizon visual planning with goal-conditioned hierarchical predictors. In Hugo Larochelle, Marc'Aurelio Ranzato, Raia Hadsell, Maria-Florina Balcan, and Hsuan-Tien Lin (eds.), *Advances in Neural Information Processing Systems 33: Annual Conference on Neural Information Processing Systems 2020, NeurIPS 2020, December 6-12, 2020, virtual*, 2020. URL https://proceedings.neurips.cc/paper/2020/hash/c8d3a760ebab631565f8509d84b3b3f1-Abstract.html.

Daniel Ratner and Manfred K. Warmuth. Finding a shortest solution for the N $\times$ N extension of the 15-puzzle is intractable. In Tom Kehler (ed.), *Proceedings of the 5th National Conference on Artificial Intelligence. Philadelphia, PA, USA, August 11-15, 1986. Volume 1: Science*, pp. 168–172. Morgan Kaufmann, 1986. URL http://www.aaai.org/Library/AAAI/1986/aaai86-027.php.

Stéphane Ross, Geoffrey J. Gordon, and Drew Bagnell. A reduction of imitation learning and structured prediction to no-regret online learning. In Geoffrey J. Gordon, David B. Dunson, and Miroslav Dudík (eds.), *Proceedings of the Fourteenth International Conference on Artificial Intelligence and Statistics, AISTATS 2011, Fort Lauderdale, USA, April 11-13, 2011*, volume 15 of *JMLR Proceedings*, pp. 627–635. JMLR.org, 2011. URL http://proceedings.mlr.press/v15/ross11a/ross11a.pdf.

Stuart Russell and Peter Norvig. *Artificial Intelligence: A Modern Approach*. Prentice Hall Press, USA, 3rd edition, 2009. ISBN 0136042597.

Stuart Russell and Peter Norvig. *Artificial Intelligence: A Modern Approach (4th Edition)*. Pearson, 2020. ISBN 9780134610993. URL http://aima.cs.berkeley.edu/.

Sartaj Sahni. Computationally related problems. *SIAM J. Comput.*, 3(4):262–279, 1974. doi: 10.1137/0203021. URL https://doi.org/10.1137/0203021.

John Schulman, Filip Wolski, Prafulla Dhariwal, Alec Radford, and Oleg Klimov. Proximal policy optimization algorithms, 2017.

Zheyan Shen, Jiashuo Liu, Yue He, Xingxuan Zhang, Renzhe Xu, Han Yu, and Peng Cui. Towards out-of-distribution generalization: A survey. *CoRR*, abs/2108.13624, 2021. URL https://arxiv.org/abs/2108.13624.

David Silver, Aja Huang, Chris J. Maddison, Arthur Guez, Laurent Sifre, George van den Driessche, Julian Schrittwieser, Ioannis Antonoglou, Vedavyas Panneershelvam, Marc Lanctot, Sander Dieleman, Dominik Grewe, John Nham, Nal Kalchbrenner, Ilya Sutskever, Timothy P. Lillicrap, Madeleine Leach, Koray Kavukcuoglu, Thore Graepel, and Demis Hassabis. Mastering the game of go with deep neural networks and tree search. *Nat.*, 529(7587):484–489, 2016. doi: 10.1038/NATURE16961. URL https://doi.org/10.1038/nature16961.

David Silver, Thomas Hubert, Julian Schrittwieser, Ioannis Antonoglou, Matthew Lai, Arthur Guez, Marc Lanctot, Laurent Sifre, Dharshan Kumaran, Thore Graepel, Timothy Lillicrap, Karen Simonyan, and Demis Hassabis. A general reinforcement learning algorithm that masters chess, shogi, and go through self-play. *Science*, 362(6419):1140–1144, 2018. doi: 10.1126/science.aar6404. URL https://www.science.org/doi/abs/10.1126/science.aar6404.

David Singmaster. *Notes on Rubik's Magic Cube*. Enslow Publishers, 1981.

Temple F Smith and Michael S Waterman. Identification of common molecular subsequences. *Journal of molecular biology*, 147(1):195–197, 1981.

Pei Sun, Henrik Kretzschmar, Xerxes Dotiwalla, Aurelien Chouard, Vijaysai Patnaik, Paul Tsui, James Guo, Yin Zhou, Yuning Chai, Benjamin Caine, Vijay Vasudevan, Wei Han, Jiquan Ngiam, Hang Zhao, Aleksei Timofeev, Scott Ettinger, Maxim Krivokon, Amy Gao, Aditya Joshi, Yu Zhang, Jonathon Shlens, Zhifeng Chen, and Dragomir Anguelov. Scalability in perception for autonomous driving: Waymo open dataset. In *2020 IEEE/CVF Conference on Computer Vision and Pattern Recognition, CVPR 2020, Seattle, WA, USA, June 13-19, 2020*, pp. 2443–2451. Computer Vision Foundation / IEEE, 2020. doi: 10.1109/CVPR42600.2020.00252. URL https://openaccess.thecvf.com/content_CVPR_2020/html/Sun_Scalability_in_Perception_for_Autonomous_Driving_Waymo_Open_Dataset_CVPR_2020_paper.html.

Richard S. Sutton and Andrew G. Barto. *Reinforcement learning - an introduction*. Adaptive computation and machine learning. MIT Press, 1998. ISBN 978-0-262-19398-6. URL https://www.worldcat.org/oclc/37293240.

Richard S. Sutton, Doina Precup, and Satinder Singh. Between mdps and semi-mdps: A framework for temporal abstraction in reinforcement learning. *Artif. Intell.*, 112(1-2):181–211, 1999. doi: 10.1016/S0004-3702(99)00052-1. URL https://doi.org/10.1016/S0004-3702(99)00052-1.

Kyo Takano. Self-supervision is all you need for solving rubik's cube. *Trans. Mach. Learn. Res.*, 2023, 2023. URL https://openreview.net/forum?id=bnBeNFB27b.

Trieu Trinh, Yuhuai Wu, Quoc Le, He He, and Thang Luong. Solving olympiad geometry without human demonstrations. *Nature*, 2024. doi: 10.1038/s41586-023-06747-5.

Aäron van den Oord, Oriol Vinyals, and Koray Kavukcuoglu. Neural discrete representation learning. In Isabelle Guyon, Ulrike von Luxburg, Samy Bengio, Hanna M. Wallach, Rob Fergus, S. V. N. Vishwanathan, and Roman Garnett (eds.), *Advances in Neural Information Processing Systems 30: Annual Conference on Neural Information Processing Systems 2017, December 4-9, 2017, Long*

*Beach, CA, USA*, pp. 6306–6315, 2017. URL https://proceedings.neurips.cc/paper/2017/hash/7a98af17e63a0ac09ce2e96d03992fbc-Abstract.html.

Joel Veness, David Silver, Alan Blair, and William Uther. Bootstrapping from game tree search. In Y. Bengio, D. Schuurmans, J. Lafferty, C. Williams, and A. Culotta (eds.), *Advances in Neural Information Processing Systems*, volume 22. Curran Associates, Inc., 2009. URL https://proceedings.neurips.cc/paper_files/paper/2009/file/389bc7bb1e1c2a5e7e147703232a88f6-Paper.pdf.

Oriol Vinyals, Igor Babuschkin, Wojciech M. Czarnecki, Michaël Mathieu, Andrew Dudzik, Junyoung Chung, David H. Choi, Richard Powell, Timo Ewalds, Petko Georgiev, Junhyuk Oh, Dan Horgan, Manuel Kroiss, Ivo Danihelka, Aja Huang, Laurent Sifre, Trevor Cai, John P. Agapiou, Max Jaderberg, Alexander Sasha Vezhnevets, Rémi Leblond, Tobias Pohlen, Valentin Dalibard, David Budden, Yury Sulsky, James Molloy, Tom Le Paine, Çaglar Gülçehre, Ziyu Wang, Tobias Pfaff, Yuhuai Wu, Roman Ring, Dani Yogatama, Dario Wünsch, Katrina McKinney, Oliver Smith, Tom Schaul, Timothy P. Lillicrap, Koray Kavukcuoglu, Demis Hassabis, Chris Apps, and David Silver. Grandmaster level in starcraft II using multi-agent reinforcement learning. *Nat.*, 575(7782):350–354, 2019. doi: 10.1038/S41586-019-1724-Z. URL https://doi.org/10.1038/s41586-019-1724-z.

Homer Walke, Kevin Black, Abraham Lee, Moo Jin Kim, Max Du, Chongyi Zheng, Tony Zhao, Philippe Hansen-Estruch, Quan Vuong, Andre He, Vivek Myers, Kuan Fang, Chelsea Finn, and Sergey Levine. Bridgedata v2: A dataset for robot learning at scale. In *Conference on Robot Learning (CoRL)*, 2023.

Yuhuai Wu, Albert Jiang, Jimmy Ba, and Roger Baker Grosse. {INT}: An inequality benchmark for evaluating generalization in theorem proving. In *International Conference on Learning Representations*, 2021. URL https://openreview.net/forum?id=O6LPudowNQm.

Zhaoyang Yang, Kathryn E. Merrick, Lianwen Jin, and Hussein A. Abbass. Hierarchical deep reinforcement learning for continuous action control. *IEEE Trans. Neural Networks Learn. Syst.*, 29(11):5174–5184, 2018. doi: 10.1109/TNNLS.2018.2805379. URL https://doi.org/10.1109/TNNLS.2018.2805379.

Ryo Yonetani, Tatsunori Taniai, Mohammadamin Barekatain, Mai Nishimura, and Asako Kanezaki. Path planning using neural a* search. In Marina Meila and Tong Zhang (eds.), *Proceedings of the 38th International Conference on Machine Learning, ICML 2021, 18-24 July 2021, Virtual Event*, volume 139 of *Proceedings of Machine Learning Research*, pp. 12029–12039. PMLR, 2021. URL http://proceedings.mlr.press/v139/yonetani21a.html.

Michal Zawalski, Michal Tyrolski, Konrad Czechowski, Tomasz Odrzygózdz, Damian Stachura, Piotr Piekos, Yuhuai Wu, Lukasz Kucinski, and Piotr Milos. Fast and precise: Adjusting planning horizon with adaptive subgoal search. In *The Eleventh International Conference on Learning Representations, ICLR 2023, Kigali, Rwanda, May 1-5, 2023*. OpenReview.net, 2023. URL https://openreview.net/pdf?id=7JsGYvjE88d.

Jiakai Zhang and Kyunghyun Cho. Query-efficient imitation learning for end-to-end simulated driving. In *Proceedings of the Thirty-First AAAI Conference on Artificial Intelligence*, AAAI'17, pp. 2891–2897. AAAI Press, 2017.

# Appendix

## Table of Contents

**A Environments** **22**

**B Key Factors For Hierarchical Search** **24**
B.1 Learning from diverse data sources . . . 24
B.2 Value Approximation Errors . . . 25
B.3 Complex Action Spaces . . . 28
B.4 Dead Ends . . . 29

**C Network Architectures & Training Details** **31**

**D Offline Pretraining** **33**
D.1 Components . . . 33
D.2 Supervised Objectives . . . 33

**E Offline Pretraining: Trajectories** **34**
E.1 Rubik's Cube . . . 34
E.2 INT . . . 34
E.3 N-Puzzle . . . 34
E.4 Sokoban . . . 34

**F Algorithms** **35**
F.1 Best-First Search . . . 35
F.2 Monte Carlo Tree Search . . . 37
F.3 A* Search . . . 39
F.4 kSubS And AdaSubS . . . 41
F.5 HIPS And HIPS-$\varepsilon$ . . . 42
F.6 Wall times . . . 43

**G Statistical Analysis Of High-Level And Low-Level Algorithms** **44**

**H Hierarchical Search** **45**

**I Further Discussion On HIPS Results** **46**

**J Common Pitfalls In Hierarchical Search evaluations** **47**
J.1 Complete Search Budget . . . 47
J.2 Baselines . . . 47
J.3 Code Quality . . . 48

**K Proof Of The Search Advancement formula** **50**

**L Proof Of The Densification Of The Action Space Theorem** **51**

## A Environments

**Sokoban** Sokoban is a classic puzzle game where the objective is to push boxes onto target locations within a confined space. It is a popular testing ground for classical planning methods and deep-learning approaches due to its combinatorial complexity and difficulty in finding solutions. Recognized as a PSPACE-hard problem, Sokoban is used to evaluate different computational strategies. Our experiments use $12 \times 12$ Sokoban boards with four boxes to assess the performance of our proposed models. An illustrative example of a simple Sokoban search tree with a solving path is shown in Figure 16.

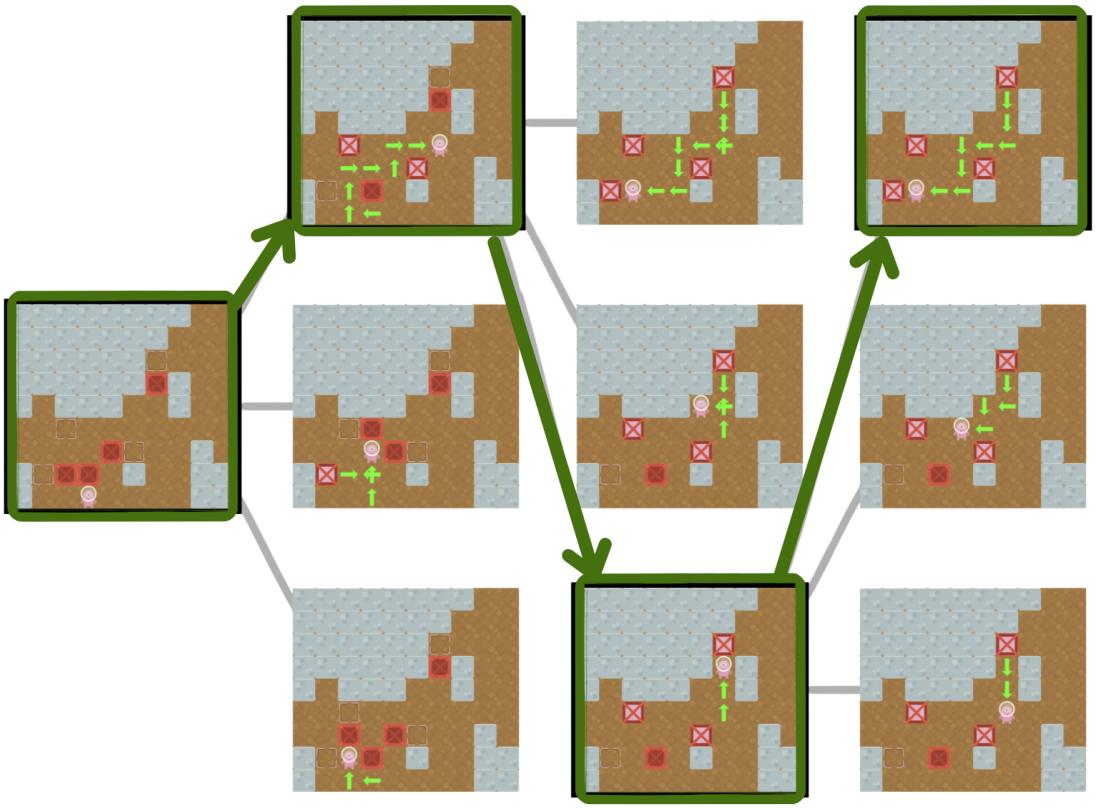

Figure 16: Hierarchical Search applied to solving Sokoban. This tree, depicted in figures, employs bolded green arrows to highlight selected subgoals within a hierarchical search framework earmarked for subsequent exploration. The illustration demonstrates that these intermediate goals exhibit variability in terms of both their spatial distance and the methodology by which a planning algorithm may leverage them.

**Rubik's Cube** The Rubik's Cube, a renowned 3D puzzle, has over $4.3 \times 10^{19}$ possible configurations, highlighting the huge search space and the computational challenge it poses. Recent advancements in solving the Rubik's Cube with neural networks underscore the potential of deep learning methods in navigating complex, high-dimensional puzzles. For the exact representation of the Rubik's Cube state, see Figure 17.

**N-Puzzle** The N-Puzzle, a classic sliding puzzle game, comes in various sizes, including the 3x3 (8-puzzle), 4x4 (15-puzzle), and 5x5 (24-puzzle). The goal is to rearrange a frame of numbered square tiles into a specific pattern, a task that tests the algorithm's ability to plan and execute a sequence of moves efficiently. Figure 18 shows a visualization of a trajectory in 24-puzzle.

**INT** INT (INequality Theorem proving) is an automated theorem-proving benchmark for high school algebraic inequality proofs. (Wu et al., 2021) provides a generator of mathematical inequalities and a proof verification tool. Each action in INT maps to a proof step, which specifies a chosen axiom and its input

| | | |
|---|---|---|
| wbrwyggwwoboybygbryrorroboygrbggbggbwybrooogrywrowywwy | $s_0$ | Initial State |
| wbrwyggggobwybwgbgooyrroyrbrrbwgbygbwybrooogroyrowywwy | $s_1$ | One Action (= single rotation) |
| wbywyoggbobwybwgbgoorrryyryywrggrbbbgybgoorgroyoowrwww | $s_2$ | |
| gyowyoggbwbwwbwwbgoorrryyryywwggbbbyboryoggroyoowrbrr | $s_3$ | |
| ... | | |
| yyyyyyyyybbbbbbrrrrrrrrggggggggooooooooobbbwwwwwwwww | $s_{n-1}$ | |
| yyyyyyyyybbbbbbbbbrrrrrrrrggggggggooooooooowwwwwwwww | $s_n$ | Solving State |

Figure 17: Example trajectory of Rubik starting from initial state $s_0$ leading to the final solution $s_n$.

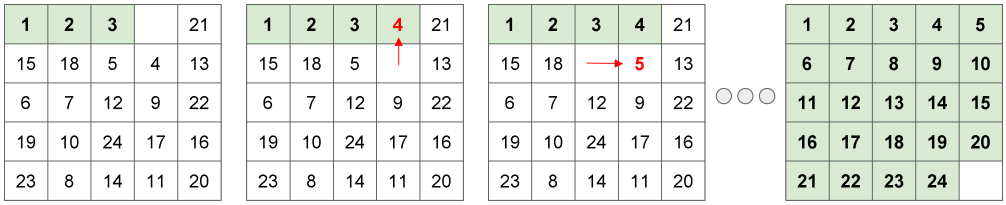


Figure 18: Example trajectory of n-puzzle starting from initial state $s_0$ leading to the final solution $s_n$. Red arrows indicate low-level actions.

entities - which makes action space very high-dimensional, enabling up to a million valid actions at a step. This large action space makes INT a desirable but challenging environment for expanding HRL paradigms to vast action spaces.

We used 25-step proofs for this paper, representing an uplift from 15 considered in (Czechowski et al., 2021; Zawalski et al., 2023) (the latter used longer proofs, but only for evaluating 15-trained models). Each step is an application of an axiom to an axiom-specific number of entities (entities are bracketed or bracketable parts of the theorem's goal).

**Example Theorems for INT environment**

**Theorem 1 Premises:** $((c + c) + d) \geq a$;
$(d + e) \geq 0$;
$((c + c) + f) \geq (0 + a)$;
$(b + g) \geq 0$;
**Goal:** $(((((((c + c) + (c + c)) \cdot 4c) + ((c + c) + d)) + (d + e)) + ((c + c) + f)) + (b + g))$
$\geq ((((0 + a) + 0) + (0 + a)) + 0)$
**Theorem 2 Goal:** $(((0 + b) + c) + a) \geq (0 + (0 + (b + (c + a))))$
**Theorem 3 Premises:** $(a + d) \geq 0$;
$(a + e) \geq (c \cdot c)$;
$(e + f) \geq 0$;
$(c + g) \geq 0$;
$(c + h) \geq (c + g)$;
$(c + i) \geq 0$;
**Goal:** $(((((((c \cdot c) \cdot (a + d)) + (a + e)) \cdot (e + f)) \cdot (c + g)) + (c + h)) \cdot (c + i))$
$\geq ((((((0 \cdot (a + d)) + (c \cdot c)) \cdot (e + f)) \cdot (c + g)) + (c + g)) \cdot (c + i))$

Figure 19: A comprehensive representation of theorems pertaining to goal achievement in mathematical expressions, showcasing the logical structure and underlying premises leading to the formulated goals.

# B Key Factors For Hierarchical Search

According to our experiments, the attributes pivotal for leveraging the advantages of high-level search include:

- learning from diverse data sources,
- hard-to-learn value function,
- complex action space,
- presence of dead ends

In Section 5, we show our main experiments that support our findings. In this appendix, we present an extended analysis of each property.

## B.1 Learning from diverse data sources

Achieving superhuman performance in complex tasks, as demonstrated by AlphaGo Silver et al. (2016), often involves large-scale datasets of demonstrations obtained from agents with varying skill levels and strategies. However, this diversity introduces challenges such as inconsistencies in demonstrations and variations in quality (Fu et al., 2020; Chen et al., 2021; Levine et al., 2020). Widely used datasets like D4RL (Fu et al., 2020), Open X-Embodiment (Collaboration et al., 2023), or Waymo Open Dataset (Sun et al., 2020) reflect this diversity, highlighting the need to address these challenges effectively. We want to answer the question whether such setting is handled better by high-level or low-level search algorithms.

**Experiment setup** For this analysis, we focus on the Rubik's cube environment. We collected a dataset of 500 000 trajectories, computed with four different solvers for the Rubik's cube:

- Beginner – the simplest human-oriented solving algorithm. It aims to order the cube layer by layer with a few primitive tactics. Because of that the solutions are structured, but also very long (typically between 150 and 200 moves).
- CFOP – an algorithm designed for speedcubers. It is based on the same principle as Beginner, but employs many advanced tactics that make the solutions faster (typically about 100 moves).
- Kociemba – a computational solver that finds near-optimal solutions (usually between 20 and 40 moves) in short time. It is heavily optimized based on the algebraic properties of the Rubik's cube.
- Random – solutions obtained by scrambling an ordered cube with random moves and reversing the trajectory.

Figure 30 shows example solutions generated with each solver. Clearly, the algorithmic solvers (Beginner and CFOP) generate much longer solutions that the other methods. They are also more structured, as they are based on building patterns. The computational solver Kociemba on the other hand go directly towards the solution because its moves are carefully optimized to ensure maximal advantage. Because of that, this dataset represent a truly diverse set of demonstrations.

**Results** As shown in Figure 2, the subgoal methods outperform the low-level methods by a wide margin. While $\rho$-BestFS is comparable on small budgets, it struggles with solving most of the instances. Also, it should be noted that the performance of the subgoal methods changes only slightly compared to training on a single Random solver (Figure 4) while the low-level searches are heavily affected.

**Learned values** To find the sources of that outcome, we checked the values learned by the heuristic function. Because of the diversity introduced by combining the experts, we should expect that the estimates are subject to high uncertainty and possibly high variance.

Figure 20 shows the distribution of the learned heuristic for random fully shuffled cubes. Although most instances can be solved optimally within 20-26 moves, the estimates range from 14 to 90 steps. Furthermore,

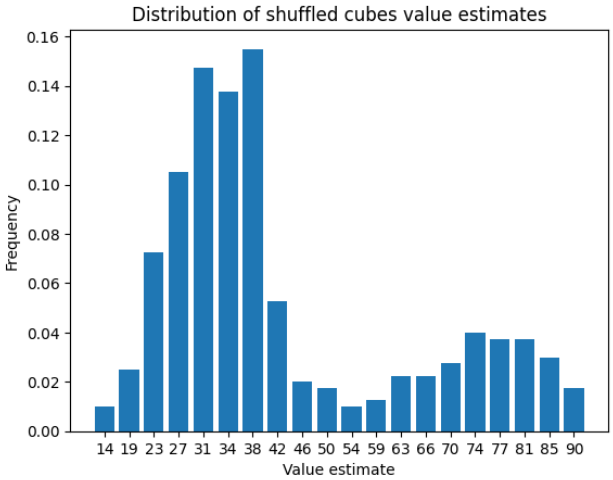


Figure 20: Value distribution for fully scrambled cubes, learned on data coming from diverse experts. The values are rescaled so that the x-axis represent the estimated number of steps to the solution. The values represent the mean of each interval.

the distribution is clearly bimodal – one mode correspond to a typical length of Kociemba solution, the other to CFOP.

Furthermore, Figure 25 shows the distribution of value estimates throughout the solutions for each solver. We observe that for the algorithmic solvers the initial distance is considerably underestimated. After about 20% moves the value network recognizes the pattern of layers built by the solvers and expect a long solution by assigning values close to 100. On the other hand, the values learned for the states visited by the computational solvers start as overestimated, but steadily decrease towards 0.

While it is a reasonable strategy for the value to fit to the provided dataset, it creates a challenge for the search. If a search algorithm aims to imitate Beginner or CFOP, it has to reach the layer pattern, characteristic of those solvers. However, the random states tend to have very low distance estimate, compared to the initial layer patterns. Because of that, for tens of steps the heuristic estimates would be actually increasing, making the reached states less and less probable to expand.

In practice, the low-level searches usually fail to cross this gap. On the other hand, the high-level methods are partially guided by the subgoal generators that ignore the values. The value gap that spans across about 30 steps can be crossed with as few as 5 subgoals of length 6. Because of that both kSubS and AdaSubS can successfully leverage the schematic algorithmic solutions.

To finally confirm that conclusion, we must answer the question whether the performance of low-level searches would increase if they could leverage the algorithmic solutions as well. For that purpose, we trained the components for each method using data only from the Beginner solver. This way we remove the challenge of noisy initial values. As shown in Figure 5, the low-level searches indeed perform much better. BestFS even matches the performance of AdaSubS. That confirms our observation that low-level searchas fail to utilize multimodal data because they rely too much on the value function and seek monotonic slopes.

At the same time we observe that since BestFS and AdaSubS show nearly identical performance on Beginner solutions, it is questionable that hierarchical methods handle long-horizon tasks better, which is a common belief (Nachum et al., 2018; Eysenbach et al., 2019; Chen et al., 2024).

### B.2 Value Approximation Errors

In many practical scenarios, value function estimates are based on either limited data samples or hand-crafted heuristics (Campbell et al., 2002; Mnih et al., 2015; Walke et al., 2023). This often leads to high

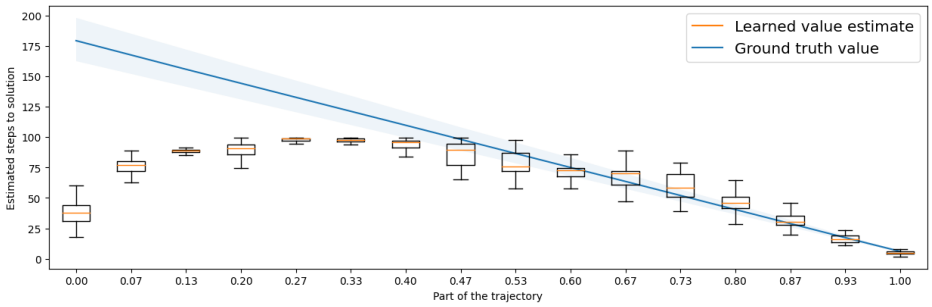


Figure 21: Beginner solver

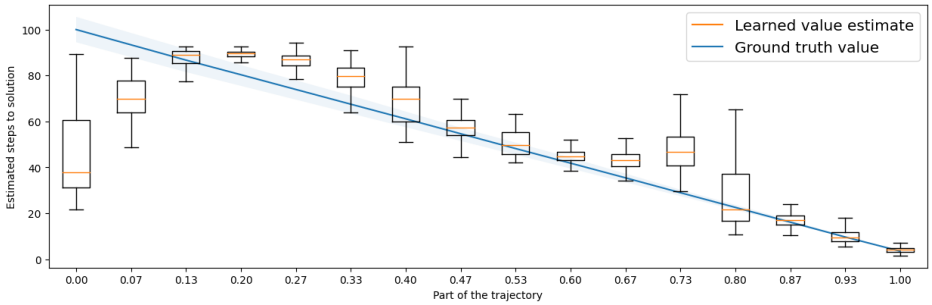


Figure 22: CFOP solver

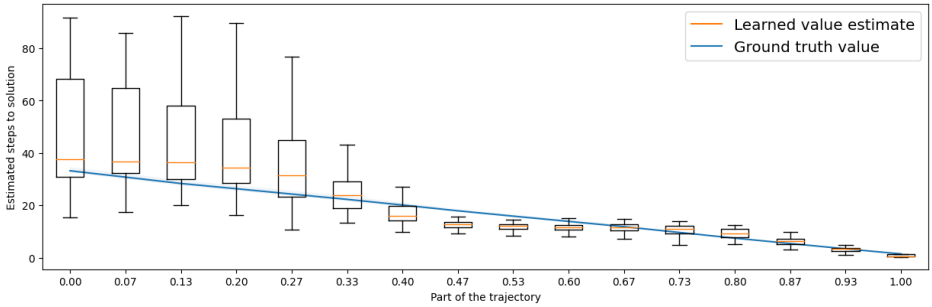


Figure 23: Kociemba solver

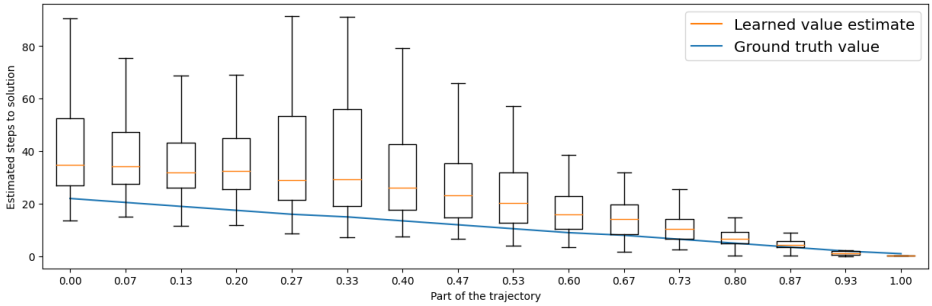


Figure 24: Reversed random 20-move trajectories

Figure 25: The learned value estimates distribution for various solvers. For each plot 100 episodes were solved using the respective solver. The boxes represent the distribution of value estimates for the consecutive points of the solution. The x-axis denotes the relative part of the trajectory (i.e., 0.5 denotes the middle point in each trajectory, regardless of its length). The blue line indicates the true number of steps to the solution.

approximation errors. If search algorithms rely too heavily on these imperfect estimates, they can make poor decisions, especially in large and complex environments where accurate value estimates are even harder to obtain (Collaboration et al., 2023; Vinyals et al., 2019).

Figure 26: Beginner

Figure 27: CFOP

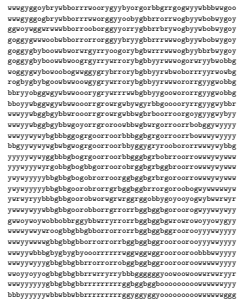

Figure 28: Kociemba

Figure 29: Random

Figure 30: Example solutions computed by each solver. Because the algorithmic solvers typically require over 100 steps, we use a tiny font to display it.

Section B.1 hints that when value estimates are subject to high uncertainty, subgoal methods should outperform low-level searches. To confirm that intuition, we run an experiment in a Rubik's cube, N-Puzzle, and Sokoban environments (Section 5.2). During inference, we add additional noise to the value estimates. That is, whenever a node is added to the search tree and its value estimate equals $\hat{v}$, we add it with the value of $\hat{v} + \mathcal{N}(0, \sigma)$ instead.

Figure 7 shows that as the amount of noise increases, each low-level method gets less and less efficient. On the extreme, when using fully random values ($\sigma = 100$), they struggle to solve any instance.

On the other hand, subgoal methods are much more resilient to noise in the value. Adaptive Subgoal Search is nearly not affected by the presence of noise. kSubS is able to retain as much as $40\% - 90\%$ success rate, even with completely random values.

Observe that the search performed by low-level methods is guided mainly by the value function. Hence, if the computed estimates are subject to high variance, low-level search struggles to make any progress. On the other hand, the subgoal search is guided both by the value function and the subgoal generator. Both the subgoal generator and the conditional policy that connects subgoals do not depend on the values. Hence, the value function is used only in the high-level nodes, which is only a fraction of the search tree.

An extreme case of that behavior is demonstrated by Adaptive Subgoal Search. Because in our configuration each generator outputs a single subgoal, the value is nearly not used at all for search. Only when the search is stuck, the secondary generators select the highest-ranked node to expand, which in this case is simply a random node of the tree. To summarize, given random value estimates, AdaSubS reduces to the following strategy:

1. Start from the root node,
2. Move from the current node to the subgoal until possible,
3. If the search is stuck, expand a random node in the search tree with a secondary generator and return to (2).

The experiments show that this simple strategy is surprisingly competitive to the greedy best-first approach, even without noise. Interestingly, it could be implemented in low-level search as well. We leave that promising experiment for future work.

### B.3 Complex Action Spaces

In environments with large action spaces, search methods often struggle due to the exponential increase in the number of choices at each decision point (Sutton & Barto, 1998). This complexity makes it difficult to efficiently identify optimal actions, slowing down decision-making and exploration (Dulac-Arnold et al., 2015; Silver et al., 2016).

The primary difference between low-level methods and subgoal methods is that the former predicts the next action, and the latter – the next state. In many environments, the action space is as simple as a few bits, allowing for iterating over all possible actions, and sampling them. At the same time, states may be considerably larger, up to the extreme of image observations. However, in some environments, the action space is comparable to the state space, or even more complex. A classic example is the AntMaze environment, in which actions are 8-dimensional, while the goal space is only 2-dimensional (Fu et al., 2020).

Among the combinatorial reasoning environments we consider, INT has the most complex action space. In INT, actions correspond to proof steps and are represented as the chosen axiom, specification of its input entities, and the required premises (Wu et al., 2021). Thus, the complexity of the action is at least comparable to the states. Moreover, solving the INT inequalities is based on constant simplification of the given expression, so the state is getting even smaller with each step.

Our experiments, shown in Figure 10, clearly confirm the advantage of using subgoal methods in the INT environment. To further verify the source of that advantage, we conducted another experiment, in a modified Rubik's cube environment. Recall that the experiment presented in Section 5.1 shows that subgoals offer no significant advantage in the *original* Rubik's cube (with a single data source). Now, we want to check whether the outcome would be different if the action space were more complex. For that purpose, we extended the action space 100 times. That is, the new action space consists of 1200 possible moves to choose from – 100 copies of each original action.

As shown in Figure 11, the subgoal methods are barely affected by the change, while the low-level searches are unable to exceed 20% success rate. That result confirms our proposition that when facing a complex action space, hierarchical methods offer considerably better performance.

According to our analysis, the primary issue with low-level searches in the augmented Rubik's cube is the lack of diversity of visited states. When for each state there are hundreds of actions that lead to a similar outcome, they are rated similarly by the policy. Hence, all the top actions essentially lead to the same outcome, which strongly limits the branching factor and trivializes the search trees. On the other hand, subgoal methods are not affected because subgoal generation does not depend on the action space. The conditional policy that connects the generated subgoals does not build a search tree, but always follows the single best action. Because of that, subgoal methods maintain their performance, even though the action space is much more complex.

It is also important to note that even though some state spaces may seem complex, the underlying manifold of possible configurations is in fact low-dimensional. For instance, we use 12x12 Sokoban boards, where each square is encoded as one-hot of 7 possible items, so technically the state space is 1008-dimensional, while there are only 4 actions. However, in practice the subgoal is defined by the positions of agent and boxes, which is at most 10-dimensional, hence rather simple to generate.

### B.4 Dead Ends

Dead-end states present a major challenge in decision-making and planning tasks. Once an agent encounters a dead end, reaching the goal becomes impossible, leading to wasted computational effort as the algorithm may continue exploring parts of the search space that do not contribute to solving the problem (Russell & Norvig, 2020). Failing to identify dead-ends may even lead to unsafe behavior (Fatemi et al., 2021; Sutton & Barto, 1998). At the same time, identifying dead-ends is NP-complete in many environments.

Specifically, a dead-end state $s$ is one from which there exists no feasible sequence of actions that leads to the goal state. Figure 31 shows an illustrative example of a dead-end state.

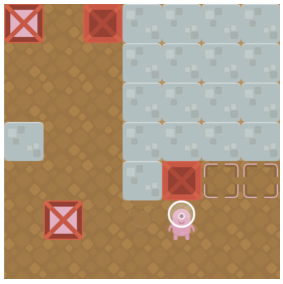

Figure 31: An example dead-end in Sokoban – a box that is pushed to the corner cannot be moved anymore, so the objective is not possible to achieve.

#### B.4.1 Examples Of Dead-Ends In kSubS vs. BestFS

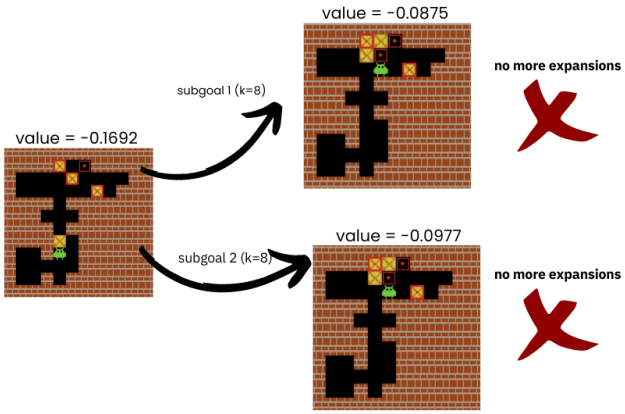


Figure 32: We illustrate a scenario where the kSubS algorithm encounters dead-ends, hindering the search process. The figure shows a case where the algorithm generates two subgoals at an expected distance (k=8), but both lead to dead-ends, wasting a portion of the search budget (18 nodes). As a result, the kSubS algorithm backtracks from this subtree and continues searching elsewhere within the tree.

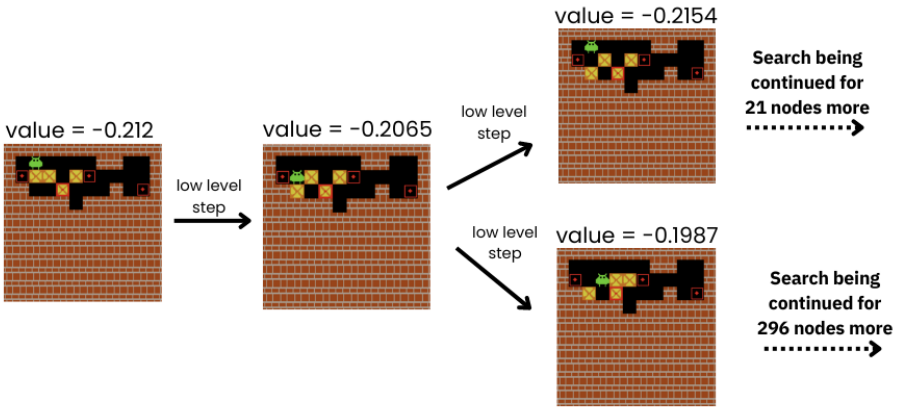


Figure 33: The figure shows BestFS expanding two nodes from a dead-end. This resulted in the exploration of over 300 additional nodes from that state, ultimately failing to find a solution within the given search budget.

In this subsection, we present examples of how each method handles dead-end situations during the search process.

For this presentation, we analyzed 128 search trees initiated from identical starting boards for both algorithms. The kSubS algorithm encountered dead-ends in 3 instances. To resolve these, it navigated through 13 high-level nodes and 105 low-level nodes within the corresponding subtrees. In contrast, the BestFS algorithm encountered dead-ends in 18 instances, requiring the traversal of 4431 nodes. Note that BestFS does not distinguish between high-level and low-level nodes in its search.

Examples of dead-end handling are shown in Figure 32 for kSubS and Figure 33 for BestFS. Observe that in the case showed in Figure 32 expanding the parent node resulted in adding two more dead-ends to the search tree. Because they have higher values, they were immediately expanded. However, the subgoal generator understood that the only way to reach solution is to make an invalid transition of releasing the blocked box. Such subgoals cannot be achieved by the conditional policy, hence no more subgoal was created in that branch. On the other hand, low-level search is unable to propose invalid transitions, so it stays in dead-end until the value estimates are higher than for other branches.

## C Network Architectures & Training Details

| Environment | Hyperparameter | Generator | CLLP | Value | Policy |
|---|---|---|---|---|---|
| INT | learning rate | 0.0001 | 0.0001 | 0.0003 | 0.0001 |
| | learning rate scheduling | linear | linear | linear | linear |
| | warmup steps | 4000 | 4000 | 2000 | 4000 |
| | batch size | 32 | 32 | 128 | 32 |
| | weight decay | 1e-05 | 1e-05 | 1e-05 | 1e-05 |
| | dropout | 0.1 | 0.1 | 0 | 0.1 |
| Rubik's Cube | learning rate | 0.0001 | 0.0005 | 3e-7 | 0.0001 |
| | learning rate scheduling | linear | linear | linear | linear |
| | warmup steps | 5000 | 50000 | 50000 | 1000 |
| | batch size | 512 | 5000 | 5000 | 2048 |
| | weight decay | 0.0001 | 0.001 | 0.00001 | 0.0001 |
| | dropout | 0.1 | 0 | 0 | 0 |
| Sokoban | learning rate | 0.00001 | 0.0001 | 0.0001 | 0.0001 |
| | learning rate scheduling | linear | linear | linear | linear |
| | warmup steps | 2500 | 1000 | 1000 | 1000 |
| | batch size | 512 | 2048 | 2048 | 2048 |
| | weight decay | 0.0001 | 0.0001 | 0.0001 | 0.000001 |
| | dropout | 0 | 0.1 | 0 | 0 |
| N-Puzzle | learning rate | 0.0001 | 0.0001 | 0.0001 | 0.0001 |
| | learning rate scheduling | linear | linear | linear | linear |
| | warmup steps | 5000 | 2000 | 2000 | 2000 |
| | batch size | 4096 | 4096 | 512 | 4096 |
| | weight decay | 0.00001 | 0.00001 | 0.00001 | 0.0001 |
| | dropout | 0.1 | 0 | 0 | 0 |

Table 1: Training-related hyperparameter values

We used BART (Lewis et al., 2020) and BERT (Devlin et al., 2019) architectures from HuggingFace Transformers for all components. Subgoal generators and INT's policies (CLLP and baseline policy) use BART. The remaining policies and value functions use BERT. Following the practice in (Zawalski et al., 2023), we've reduced model size parameters, as detailed in Table 2.

**INT** As states in INT are complex objects, we prefer to use their string representations and avoid mapping arbitrarily generated strings into complex states. Requisite modifications to the component definition are best illustrated analogously to D.1. A generator is redefined as follows:

$$\mathcal{G}_{\text{int}} : \underbrace{\mathcal{S}}_{\text{state to expand}} \rightarrow \underbrace{P(\mathcal{T})}_{\text{set of } \textit{proposed} \text{ subgoals (in string format)}}$$

and conditional level policy:

$$\mathcal{P}_{\text{int}} : \underbrace{\mathcal{S}}_{\text{current state}} \times \underbrace{\mathcal{T}}_{\text{subgoal } \textit{representation}} \rightarrow \underbrace{\mathcal{A}}_{\text{action}}$$

**Sokoban** Unlike prior work (Zawalski et al., 2023; Czechowski et al., 2021), which used convolutional networks for all components, we work on tokenized representations of Sokoban boards and use BERT/BART architectures instead. This modification did not adversely impact our ability to replicate AdaSubS and kSubS results.

**Training pipeline** We trained our models from scratch using the HuggingFace Transformer pipeline. Detailed training parameters, which varied across environments, can be found in 1.

**Infrastructure** For training, we used a single NVIDIA A100 40GB GPU node, and each component's training took up to 48 hours. Because we used pre-trained trajectories, we did not need to use more than

one core during training. We ran an evaluation using 24-core CPU jobs on Xeon Platinum 8268 nodes with 192GB of memory.

| Environment | Hyperparameter | Generator | CLLP | Value | Policy |
|---|---|---|---|---|---|
| INT | d model | 512 | 512 | - | 512 |
| | decoder layers | 6 | 6 | - | 6 |
| | intermediate size | - | - | 256 | - |
| | encoder attention heads | 8 | 8 | - | 8 |
| | hidden size | - | - | 128 | - |
| | num hidden layers | - | - | 2 | - |
| | decoder ffn dim | 2048 | 2048 | - | 2048 |
| | encoder ffn dim | 2048 | 2048 | - | 2048 |
| | encoder layers | 6 | 6 | - | 6 |
| | decoder attention heads | 8 | 8 | - | 8 |
| Sokoban | d model | 256 | - | - | - |
| | decoder layers | 3 | - | - | - |
| | intermediate size | - | 512 | 128 | 512 |
| | encoder attention heads | 4 | - | - | - |
| | hidden size | - | 512 | 128 | 512 |
| | num hidden layers | - | 6 | 1 | 6 |
| | encoder ffn dim | 2048 | - | - | - |
| | decoder ffn dim | 1024 | - | - | - |
| | encoder layers | 3 | - | - | - |
| | decoder attention heads | 4 | - | - | - |
| N-Puzzle | d model | 64 | - | - | - |
| | decoder layers | 3 | - | - | - |
| | intermediate size | - | 128 | 128 | 256 |
| | encoder attention heads | 4 | - | - | - |
| | hidden size | - | 128 | 128 | 256 |
| | num hidden layers | - | 2 | 1 | 3 |
| | encoder ffn dim | 64 | - | - | - |
| | decoder ffn dim | 64 | - | - | - |
| | encoder layers | 3 | - | - | - |
| | decoder attention heads | 4 | - | - | - |
| Rubik's Cube | d model | 256 | - | - | - |
| | decoder layers | 3 | - | - | - |
| | intermediate size | - | 512 | 128 | 512 |
| | encoder attention heads | 4 | - | - | - |
| | hidden size | - | 512 | 128 | 512 |
| | num hidden layers | - | 2 | 1 | 6 |
| | encoder ffn dim | 2048 | - | - | - |
| | decoder ffn dim | 1024 | - | - | - |
| | encoder layers | 3 | - | - | - |
| | decoder attention heads | 4 | - | - | - |

Table 2: Model-related hyperparameter values

# D Offline Pretraining

Models are pretrained using an offline imitation learning approach. Specifically, given a set of solution trajectories $\{(s_0, s_1, \ldots, s_{n_i})\}_{i=1}^{N}$ produced by an expert $\mathcal{M}$, or multiple experts $\{\mathcal{M}_j\}_{j=1}^{M}$ in cases where offline trajectories are collected from multiple experts, the objective is to learn from these trajectories. It is important to note that these trajectories are not required to be optimal; they may include loops or numerous redundant actions. Description of all components can be found in section $D.1$ and supervised training objectives in section $D.2$.

## D.1 Components

During the pretraining phase, models undergo an offline imitation learning process. Specifically, they are trained on a set of solution trajectories $\{(s_0, s_1, \ldots, s_{n_i})\}_{i=1}^{N}$, which are collected to facilitate the learning of decision-making strategies.

**Generator** The generator component is responsible for generating subgoal propositions upon receiving a state. These propositions are designed to facilitate progress toward the solution by suggesting intermediate steps that direct the search process more efficiently.

$$\mathcal{G}: \underbrace{\mathcal{S}}_{\text{state to expand}} \rightarrow \underbrace{P(\mathcal{S})}_{\text{set of subgoal propositions}}$$

**Conditional Low-Level Policy** The Conditional Low-Level Policy (CLLP) plays a crucial role in node expansion by evaluating each subgoal proposition. For a given current state and a subgoal, the CLLP recommends actions that lead toward achieving the subgoal. A path from the current node to the subgoal is constructed through the iterative execution of these actions. Subgoals reached within a predefined number of steps, $k$, are incorporated into the graph, while those that are not are discarded.

$$\mathcal{P}: \underbrace{\mathcal{S}}_{\text{current state}} \times \underbrace{\mathcal{S}}_{\text{subgoal state}} \rightarrow \underbrace{\mathcal{A}}_{\text{action}}$$

**Value** The value function estimates the distance from a current state to the final solution. This estimation is used to guide the selection and expansion of nodes, influencing the overall search strategy.

$$\mathcal{V}: \underbrace{\mathcal{S}}_{\text{state to evaluate}} \rightarrow \underbrace{\mathbb{R}}_{\text{value of the state}}$$

**Behavioral Cloning Policy** The policy $\Pi_{\text{BC}}$ is a decision-making function that maps the current state to an action. It encapsulates the strategy derived from the learning process, guiding the agent's actions towards achieving the final goal.

$$\Pi_{\text{BC}}: \underbrace{\mathcal{S}}_{\text{current state}} \rightarrow \underbrace{\mathcal{A}}_{\text{action}}$$

## D.2 Supervised Objectives

Each expert trajectory is defined as a sequence of states and corresponding actions $(s_0, a_0), \ldots, (s_{n-1}, a_{n-1}), s_n$ that delineate a path to a solution. The training methodology leverages this data through several key self-supervised imitation mappings:

- A $k$-subgoal generator that maps a state $s_i$ to a future state $s_{i+k}$, simulating the achievement of intermediate goals.
- A value function that estimates the remaining steps to the solution by mapping state $s_i$ to a numerical value $(i - n)$, representing the estimated distance from the goal.
- A policy that maps each state-action pair $(s_i, s_{i+d})$, with $d \leq k$, to the corresponding action $a_i$, thereby guiding the decision-making process towards the solution.

# E Offline Pretraining: Trajectories

## E.1 Rubik's Cube

### E.1.1 Random

To construct a random successful trajectory, we performed 20 random permutations on an initially solved Rubik's Cube and took the reverse of this sequence, replacing each move with its reverse. Such solutions are usually sub-optimal since random moves are not guaranteed to increase the distance from the solution. They can even make loops in the trajectories. However, a cube scrambled with 20 moves is usually close to a random state, so such trajectories give a decent space coverage.

### E.1.2 Beginner, CFOP

*Beginner* and *CFOP* are algorithms commonly used by humans. They solve the cube by ordering the stickers layer by layer. Because of that, the solutions are highly structured and long – usually between 100 and 200 moves. Both algorithms are composed of several subroutines that help building the consecutive layers. Thus, the structure of such solutions highly resembles the subgoal search.

### E.1.3 Kociemba

The *Kociemba two-stage solver* leverages the algebraic structure of the Rubik's Cube. In the first stage, its goal is to enter a specific subgroup. Since that subgroup is much smaller than the whole space, completing the solution may be done efficiently. *Kociemba* finds reasonably short solutions (usually between 20 and 40 moves) and works reasonably fast.

### E.1.4 Size Of Datasets

For training the components on a dataset collected by a single solver, we generate 100 000 trajectories. For the experiment with diverse experts, each solver generates 25 000 trajectories for a total of 100 000.

## E.2 INT

Trajectories are constructed from sequences of axiom applications, similarly to (Zawalski et al., 2023), who followed (Wu et al., 2021). A set of up to 15 (out of 18) axioms is first selected, and then a random axiom order is set and validated. Finally, a proof is converted to a relevant trajectory. Approximately 500,000 trajectories were generated for model pre-training.

We capped the number of axioms at 15 because some pairs of axioms (eg. terminal axioms) cannot be in one trajectory.

## E.3 N-Puzzle

To collect data for N-puzzles, we utilized an algorithm that initially arranges block number 1, followed by block number 2, and so forth, as depicted in Figure 18. The training set comprises approximately $10,000$ trajectories.

## E.4 Sokoban

To collect trajectories for Sokoban, we used a trained MCTS agent that gathered approximately $100,000$ trajectories.

# F Algorithms

## F.1 Best-First Search

**Overview** Best-First Search greedily prioritizes node expansions with the highest heuristic estimates, aiming for paths that likely lead to the goal. While not ensuring optimality, BestFS provides a simple yet efficient strategy for navigating complex search spaces. The high-level pseudocode for BestFS is outlined in Algorithm 1, and the detailed pseudocode is presented in Algorithm 2.

**Algorithm 1** Pseudocode for Best-First Search

```
while has nodes to expand do
    Take node N with the highest value
    Select children n_i of N
    Compute values v_i for the children
    Add (n_i, v_i) to the search tree
end while
```

**Heuristic** In our implementation, we adhere to the Best-First Search principle by utilizing the learned value function, a common practice in the planning domain (Brunetto & Trunda, 2017; Czechowski et al., 2021; Zawalski et al., 2023; Kujanpää et al., 2023a). It should be noted that in each of our experiments, all the compared algorithms use the same value function network. This way we ensure that the differences come solely from the algorithmic part.

**Selecting children** When expanding a node during search, the standard BestFS algorithm adds all its children. However, in our implementation, we aimed to reduce the search tree size by selecting only the most promising children. We achieve this by sorting the children according to their probability distribution predicted by the policy network. For choosing the final subset of children, we employ two approaches. In the simpler variant, we always select the top $k$ actions. In the second variant, we add top children until their cumulative probability exceeds a fixed threshold $t_{conf}$.

This pruning does not adversely affect the standard algorithm, as nodes are still chosen based on their heuristic values, while the threshold sets a practical limit on the search space. Our results demonstrate that BestFS tends to perform much better with a confidence threshold (Figure 34). However, its performance is highly sensitive to this threshold as it balances exploration and exploitation, illustrating the impact of different confidence thresholds on success rates.

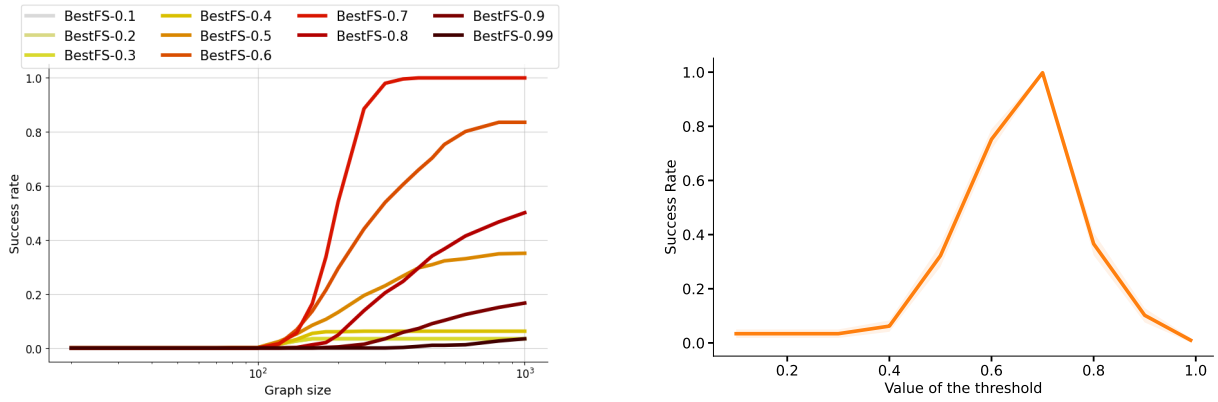


Figure 34: Comparison of success rates for the BestFS algorithm on the Rubik's Cube with various confidence threshold values. BestFS-X represents the BestFS algorithm with the confidence threshold set to X. *Left:* The plot displays the achieved success rate relative to the graph size. *Right:* The plot illustrates the success rate for a budget of 500 nodes.

**Completeness** In the Rubik's Cube environment with random trajectories, the subgoal methods solve more instances than BestFS given a low search budget, but with more resources, BestFS takes the lead (see Figure 4). Also, in other experiments, we may observe that BestFS typically requires higher computational budget to solve the simplest instances, but its performance increases considerably with more resources.

That behavior is related to the fact that the search trees built by hierarchical methods are much sparser because the branching occurs only in the high-level nodes. On the other hand, the low-level algorithms can cover a higher fraction of the space. On the extreme, if we used all the available actions for every expansion, the low-level search would be *guaranteed* to find a solution if one exists. Our mechanism of selecting the actions removes that guarantee. However, at the same time, it drastically improves performance (compare BestFS-0.7 with BestFS-0.99 which is complete), which makes it a much better choice for our study.

We note that the high-level algorithms could be made complete, as proposed in (Kujanpää et al., 2023b; Zawalski et al., 2023). However, to maximize the efficiency we choose to keep the tested algorithms in their original form. The ability to search with sparse trees not only lets the methods advance fast, but also withdraw quickly if the branch does not lead to the solution (is a dead end).

**Hyperparameters** To identify the most suitable solving parameters, we used grid search. Initially we grid over coarse values (namely 0.1, 0.2, 0.3, 0.4,0.5, 0.6, 0.7, 0.8, 0.9, and 0.99). Then we check finer values (with precision of 0.05) around the best-performing threshold. The best-performing thresholds range from 0.6 to 0.85, depending on the environment and the components that are used.

For determining the best number of top actions $k$ for the simpler variant, we simply check every possible number of actions. Usually selecting 2 actions is by far the best choice.

Details regarding hyperparameters of the networks are listed in Appendix D.1.

**Algorithm 2** Complete pseudocode for Best-First Search

```
Require:
  value function network V,
  policy ρ_BFS
  predicate of solution SOLVED

  function SEARCH(s_0)
  T ← ∅ {priority queue}
  T.PUSH((V(s_0), s_0))
  parents ← {}
  seen.ADD(s_0) {seen is a set}

  while 0 < LEN(T) and LEN(seen) < max_budget do
    _, s ← T.EXTRACTMAX() {select node with the highest value}
    actions ← ρ_BFS(s)

    for a in actions do
      s' ← ENVSTEP(s, a)

      if s' in seen then
        continue
      end if

      seen.ADD(s')
      parents[s'] ← s
      T.PUSH((V(s'), s'))

      if SOLVED(s') then
        {solution found}
        return EXTRACTLOWLEVELTRAJECTORY(s', parents)
      end if
    end for
  end while

  return False {solution not found}
```

### F.2 Monte Carlo Tree Search

**Overview** Our Monte Carlo Tree Search (MCTS) solver, designed for a single-player setting, is based on the AlphaZero framework (Silver et al., 2018). The high-level workflow of MCTS is illustrated in Figure 35, and detailed pseudocode is provided in Algorithm 3.

The algorithm's operation consists of four primary stages:

- **Selection**: The most promising node is selected using Polynomial Upper Confidence Trees (PUCT), augmented with an exploration weight to strike a balance between exploiting known strategies and investigating new pathways.
- **Expansion**: The selected node is expanded, generating new child nodes that correspond to prospective future actions. This expansion widens the search tree and enables the exploration of various outcomes.
- **Simulation**: Following the AlphaZero approach (Silver et al., 2018), policy and value networks replace traditional simulations. The policy network suggests favorable moves, while the value network predicts their probability of success, directing the algorithm towards beneficial trajectories.
- **Backpropagation**: The insights derived from the networks are used to update node values, improving future decision-making.

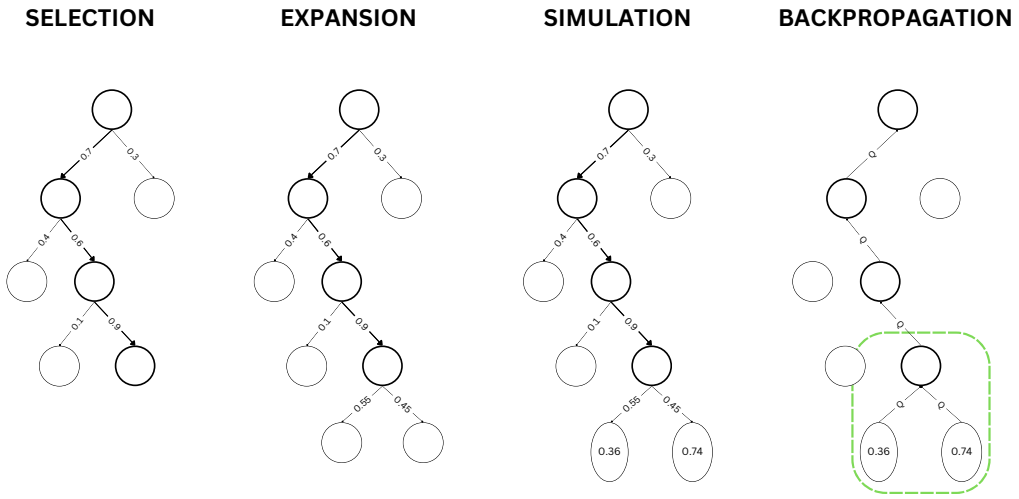


Figure 35: Schematic diagram of the MCTS algorithm in our implementation. Arrows show policy network probabilities and node values are valued network predictions. Q values, calculated via PUCT, integrate these with exploration-exploitation balance.

**Hyperparameters** In the MCTS algorithm, the parameters were set as follows: sampling temperatures were chosen from [0, 0.5, 1]. The number of steps varied between 200 and 1000, and the number of simulations ranged from 5 to 300. The discount factor and exploration weight were consistently set at 1.

**Algorithm 3** MCTS Solver

**Require:**
Number of simulations: $N_s$
Discount factor: $\gamma$
Exploration weight: $c_{\text{puct}}$
Sampling temperature: $\tau$
Value function: $V$
Environment model: $M$
Initial state: *initial_state* from env

**function** SEARCH((*initial_state*))
*root* ← *initial_state*
*iteration* ← 0
**while** *iteration* $< N_s$ **do**
  *node* ← *root*
  **while** *node* is not a leaf **do**
    *node* ← SELECTCHILD(*node*), according to PUCT formula
  **end while**
  *leaf* ← *node*
  Expand the leaf using the environment model $M$, policy $\pi$, value function $V$, and discount factor $\gamma$
  Backpropagate results through the path to update $N, W, Q$
  *iteration* ← *iteration* + 1
**end while**
*best_child* ← Sample child of the *root* according to $\tau$ and $N$
**return** action leading to *best_child*

### F.3 A* Search

**Overview** Like Best-First Search, A* prioritizes the exploration of promising nodes. However, A* strategically guides its search by incorporating both the actual cost to reach a node and a heuristic estimate of the remaining distance to the goal. This way it balances the greedy exploitation and conservative exploration. The high-level pseudocode for A* is outlined in Algorithm 4, and the detailed pseudocode is presented in Algorithm 5.

**Algorithm 4** Pseudocode for A*

```
while has nodes to expand do
    Take node N with the highest value
    Select children n_i of N
    Compute values v_i for the children
    Compute depth d_i for the children
    Add (n_i, λd_i + v_i) to the search tree
end while
```

**Heuristic** A* guidance is achieved through the following cost function:

$$f(node) = \lambda g(node) + h(node)$$

where:

- $g(node)$: The cost to reach *node* from the start state, in our case its depth in the search tree.
- $h(node)$: A heuristic estimate of the cost from *node* to the goal state.
- $\lambda$: A scaling factor balancing the influence of actual cost and heuristic estimate.

For heuristic $h$, we used a value network, like for BestFS (see Appendix F.1). If the heuristic used for A* is *admissible*, i.e. it never overestimates the cost of reaching the goal, A* is guaranteed to find an optimal solution. For instance, if we used $h(node) \equiv 0$, A* would reduce to the Dijkstra algorithm. The heuristic that we learn is not guaranteed to be admissible. Firstly, it estimates the distance according to the demonstrations, which is always an upper bound for the optimal distance. Secondly, the approximation errors introduce additional uncertainty. However, our main focus is on finding any solution, not necessarily an optimal one.

**Selecting children** During the search, A* maintains a priority queue of nodes to be explored. Similarly to BetsFS (Appendix F.1) for reducing the search tree size, we select the most promising children. At each iteration, the node with the lowest $f(node)$ value is selected for expansion. The algorithm proceeds until the goal state is reached or the computational budget is exceeded.

**Hyperparameters** The key parameter for A* is the cost weight $\lambda$. On the extreme, setting $\lambda = 0$ reduces A* to greedy BestFS, while setting $\lambda = \infty$ makes it equivalent to Breadth-First Search. By tuning that parameter, we control the trade-off between exploration and exploitation of the search.

To tune the depth parameter for our experiments, we grided over values $[0.1, 0.2, 0.5, 1, 2, 5, 10]$. However, usually the best choice was to keep the cost weight low (0.1 or 0.2, see Figure 36). While conservative search allows A* avoid more dead-ends than BestFS (see Figure 5.4), usually greedy steps lead to finding the solution much faster.

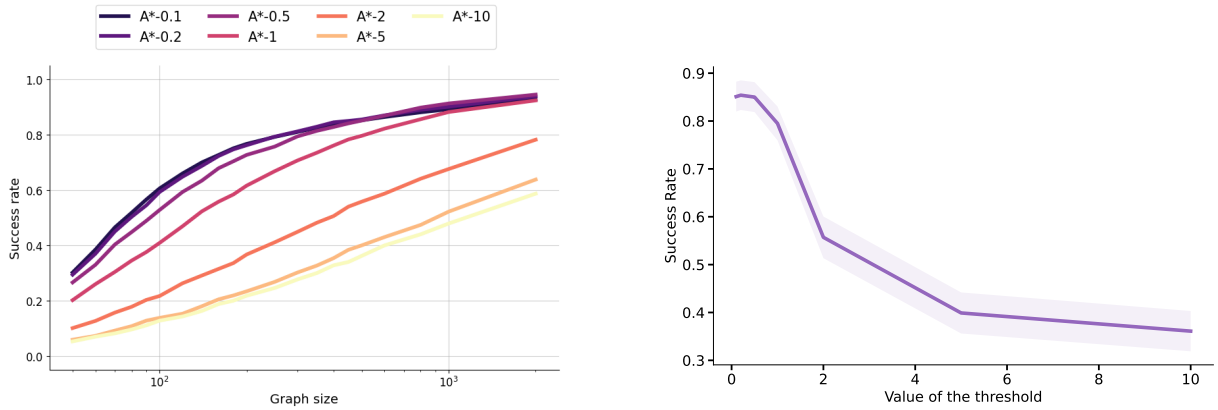


Figure 36: Figures presented above illustrate the impact of depth cost scaling on the overall success rate of the A* algorithm on Sokoban, employing a confidence threshold of 0.85. In most experiments, the smaller the depth scaling factor is, the better is the final success rate. The left figure shows the success rate curves for different choices of cost weight $\lambda$, while the right plot compares those variants for a fixed budget of 500 computation nodes.

**Algorithm 5** Complete pseudocode for $A^*$ Search

```
Require:
  value function network V
  policy ρ_BFS
  predicate of solution SOLVED
  depth scaling factor λ

  function SEARCH(s_0)
  T ← ∅ {priority queue}
  T.PUSH((V(s_0), s_0))
  parents ← {}
  seen.ADD(s_0) {seen is a set}

  while 0 < LEN(T) and LEN(seen) < max_budget do
    _, s ← T.EXTRACTMAX() {select node with the highest value}
    actions ← ρ_BFS(s)

    for a in actions do
      s' ← ENVSTEP(s, a)

      if s' in seen then
        continue
      end if

      seen.ADD(s')
      parents[s'] ← s
      T.PUSH((V(s') − λ · depth(s'), s'))

      if SOLVED(s') then
        {solution found}
        return EXTRACTLOWLEVELTRAJECTORY(s', parents)
      end if
    end for
  end while

  return False {solution not found}
```

### F.4 kSubS And AdaSubS

**Overview** AdaSubS is a hierarchical search algorithm designed to solve combinatorial problems by operating on high-level nodes, which represent multiple steps rather than single actions. It employs multiple generators $\mathcal{G}_{k_1}, \mathcal{G}_{k_2}, \ldots, \mathcal{G}_{k_m}$ to generate subsequent subgoals, a value function $\mathcal{V}$ to estimate the distance from a given state to the solution, and a conditional low-level policy $\mathcal{P}$ to execute a series of actions leading from one subgoal to the next. kSubS is a special case of AdaSubS, where only a single generator is used. These methods are introduced and studied in (Czechowski et al., 2021; Zawalski et al., 2023).

**Stages** The method begins by adding $m$ initial nodes (one per each generator) to a priority queue, where each initial node $i$ is assigned a priority $(k_i, \mathcal{V}(s_0))$. Here, $k_i$ is the length of the generator used during the node's expansion, and $\mathcal{V}(s_0)$ estimates the distance (in low-level actions) between $s_0$ and the solution. The following steps are repeated until a solution is found or the budget is exhausted:

- **Selection for expansion**: The node $((k, \mathcal{V}(s), s)$ with the highest priority is extracted from the queue. This priority structure ensures that the algorithm prioritizes expanding the longest subgoals whenever possible.
- **Generating subgoals**: The current state $s$ is passed to the selected generator $\mathcal{G}_k$, which produces multiple subgoal propositions represented as states $s_1^*, s_2^*, \ldots, s_p^*$.
- **Verifying reachability**: Since $\mathcal{G}_k$ can produce invalid or unreachable subgoals, each proposed subgoal must be verified. The conditional low-level policy $\mathcal{P}$ begins an iterative process, taking single steps from $s$ towards the proposed subgoal $s_j^*$. If $s_j^*$ is reached within $k$ steps, the subgoal is accepted, and new high-level nodes $\{\big((k_i, \mathcal{V}(s_j^*)), s_j^*\big)\}_{i \in \{1 \ldots m\}}$ are added to the priority queue as potential future subgoals to expand.

For a graphical overview of how AdaSubS works, see Appendix H.

**Algorithm 6** Complete pseudocode for Adaptive Subgoal Search

```
Require:
  C_1 max number of nodes,
  V value function network,
  ρ_{k_0}, ..., ρ_{k_m} subgoal generators,
  SOLVED predicate of solution

  function SOLVE((s_0))
  T ← ∅ {priority queue with lexicographic order}
  parents ← {}
  for k in k_0, ..., k_m do
    T.push((k, V(s_0)), s_0)
  end for
  seen.add(s_0) {seen is a set}
  while 0 < len(T) and len(seen) < C_1 do
    (k, _), s ← T.extract_max()
    subgoals ← ρ_k(s)
    for s'  in  subgoals do
      if s'  not in  seen then
        if IS_VALID(s, s') then
          seen.add(s')
          parents[s'] ← s
          for k in k_0, ..., k_m do
            T.push((k, V(s')), s')
          end for
          if SOLVED(s') then
            return EXTRACTLOWLEVELTRAJECTORY(s', parents)
          end if
        end if
      end if
    end for
  end while
  return False
```

### F.5 HIPS And HIPS-$\varepsilon$

Here we show a pseudocode for HIPS and HIPS-$\varepsilon$ methods. For details see Alg. 7

**Algorithm 7** Complete pseudocode for HIPS with BestFS-PHS* and VQ-VAE

```
Require:
  C_1 max number of nodes,
  VAE Variational Autoencoder for subgoal generation,
  SOLVED predicate of solution,
  ϵ exploration parameter for balancing,
  V value function for PHS* cost estimation

  function EXTENDED_HIPS_SOLVE((s_0))
  Initialize search data structures, including priority queues.
  seen.add(s_0) {Track seen states}
  while search conditions are met do
    Use PHS* search strategy to select a state s.
    Generate subgoals subgoals ← VAE(s).
    for each s' in subgoals do
      if s' not seen and is valid then
        Evaluate s' using V for PHS* cost.
        Update priority queue based on PHS* cost.
        if SOLVED(s') then
          return Construct solution path.
        end if
      end if
    end for
  end while
  return False {Solution not found}
```

### F.6 Wall times

In our experiments, we focus on measuring the search budget in terms of the number of visited states before finding the solution. However, it is also important to consider the total running time for completeness.

Subgoal methods introduce computational overhead. However, we note that each low-level method calls policy and value function once in every visited state, and similarly, subgoal methods also call policy and value once in every visited state. The only additional computation in subgoal methods comes from invoking the subgoal generator, which occurs in a fraction of the nodes explored. In each experiment, all methods share exactly the same heuristic function and use policies of equal size. As a result, the Complete Search Budget metric should be closely aligned with computational cost.

We opted to focus on a budget metric that is hardware-independent, reproducible, and widely applicable, ensuring that our results can serve as a reference point for future research. The Complete Search Budget answers the question "How many states must be explored before finding a solution?" rather than "How long does it take to find a solution?". These are slightly different questions, but both are relevant when assessing planner quality.

We acknowledge that we did not optimize the implementation for runtime efficiency, instead opting for the architectures used by (Czechowski et al., 2021) and (Zawalski et al., 2023) rather than optimizing computational complexity. Additionally, measuring wall-clock time introduces confounding factors, such as a bug in Hugging Face's beam search implementation that prevents decoding parallelization, introducing bias against subgoal methods.

For completeness, we report wall-clock times of each method in Table 3.

| | $\rho$-BestFS | $\rho$-A* | $\rho$-MCTS | kSubS | AdaSubS |
|---|---|---|---|---|---|
| Rubik | 26 | 26 | 153 | 214 | 96 |
| INT | 1997 | 1985 | - | 1444 | 1999 |
| Sokoban | 34 | 36 | 59 | 125 | 123 |
| NPuzzle | 27 | 32 | 29 | 40 | 39 |

Table 3: Comparison of evaluation time of search algorithms. The values express the total time of solving 500 instances, in minutes.

## G Statistical Analysis Of High-Level And Low-Level Algorithms

| Environment | Algorithm | Tree size | Number of leaves | Branching factor | Solution length | Solution length (subgoals) |
|---|---|---|---|---|---|---|
| N-Puzzle | BestFS | 354.43 | 1.34 | 1.0 | 354.08 | - |
| | A* | 354.09 | 1.34 | 1.0 | 353.56 | - |
| | MCTS | 742.04 | 371.52 | 2.0 | 347.43 | - |
| | kSubS-8 | 353.66 | 1.0 | 1.0 | 353.66 | 45.67 |
| Sokoban | BestFS | 185.24 | 36.88 | 1.22 | 48.98 | - |
| | A* | 85.04 | 12.22 | 1.43 | 45.68 | - |
| | MCTS | 255.0 | 128.0 | 2.0 | 45.1 | - |
| | kSubS-8 | 101.92 | 6.6 | 1.06 | 46.88 | 7.23 |
| Rubik's Cube | BestFS | 152.25 | 58.02 | 1.65 | 48.92 | - |
| | A* | 185.23 | 69.57 | 1.64 | 45.46 | - |
| | MCTS | 716.46 | 358.73 | 2.0 | 33.32 | - |
| | kSubS-4 | 303.52 | 133.44 | 1.12 | 73.58 | 26.65 |

Table 4: Average values of tree size, number of leaves, branching factor (average number of children), and solution length were calculated for 100 boards solved by all presented algorithms. Additionally, for the subgoal method, the average number of subgoals on the winning path was determined.

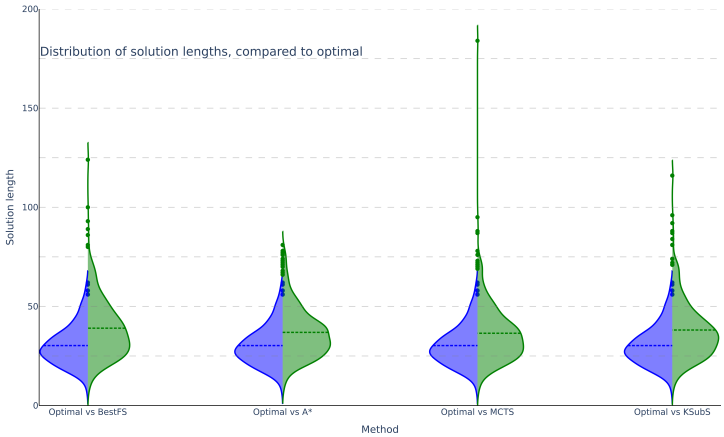


Figure 37: The distribution of solution length in Sokoban. The right part of each plot illustrates the distribution for the methods that we used. The left part corresponds to the optimal solutions for the tested instances obtained using Breadth-First Search. These algorithms were evaluated on 494 commonly solved instances.

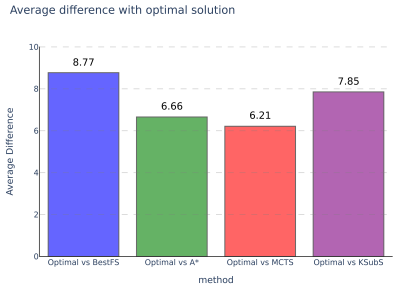


Figure 38: The average difference between the solutions found by each algorithm and the optimal solutions for the Sokoban environment. These algorithms were evaluated on 494 commonly solved instances.

## H Hierarchical Search

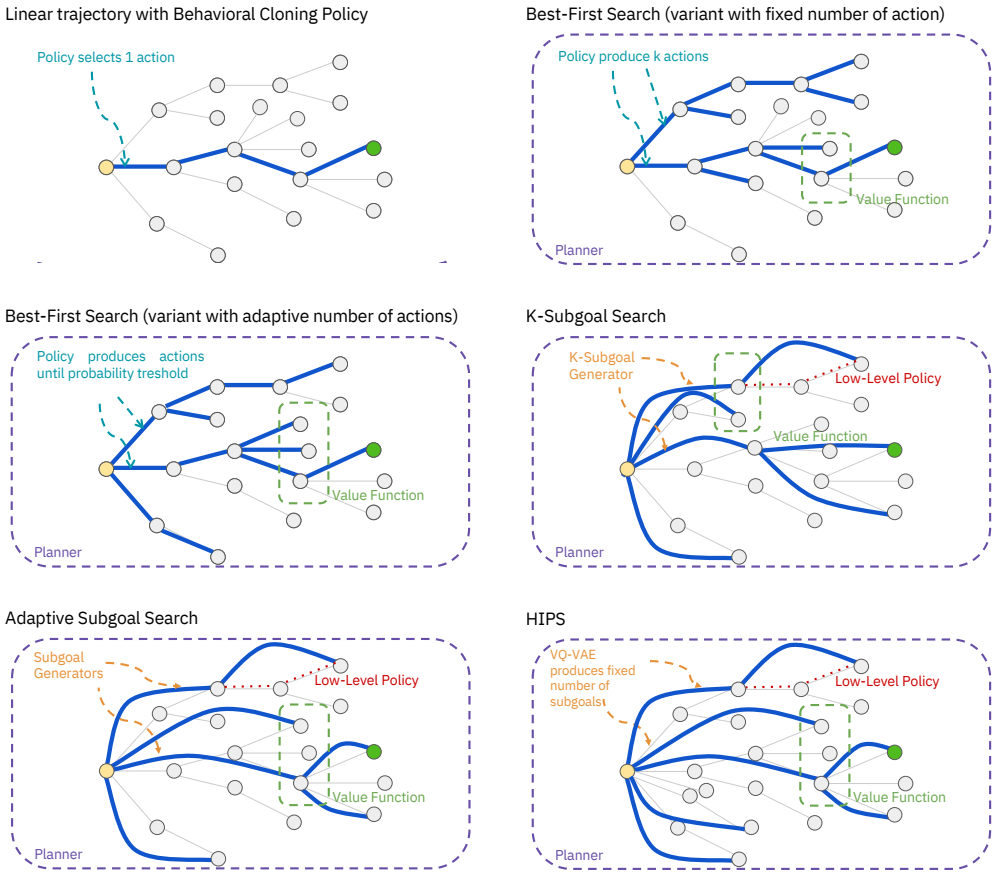


Figure 39: Overview of the search methods under consideration, accompanied by illustrative examples depicted in various plots for each method. Specifically, straight blue lines are utilized to represent low-level actions that occur within the search space. In contrast, long skip connections are used to symbolize subgoals within the search process.

# I Further Discussion On HIPS Results

HIPS and HIPS-$\varepsilon$ (Kujanpää et al., 2023a;b) are recent hierarchical search algorithms proposing to generate subgoals with variational autoencoders. We attempted to use HIPS and HIPS-$\varepsilon$ in greedy and prior-informed variations, and for all HIPS methods, the cost of inference was prohibitively high.

To compare these methods, we used A*-generated data from HIPS papers, in contrast to all other experiments (which use data generated by us).

Our evaluation, illustrated in 40, shows that HIPS uses 100x more low-level nodes in search than comparable subgoal search methods and baselines - despite relatively similar subgoal efficiency as calculated in relevant papers. These findings informed our decision not to evaluate HIPS in the rest of the paper.

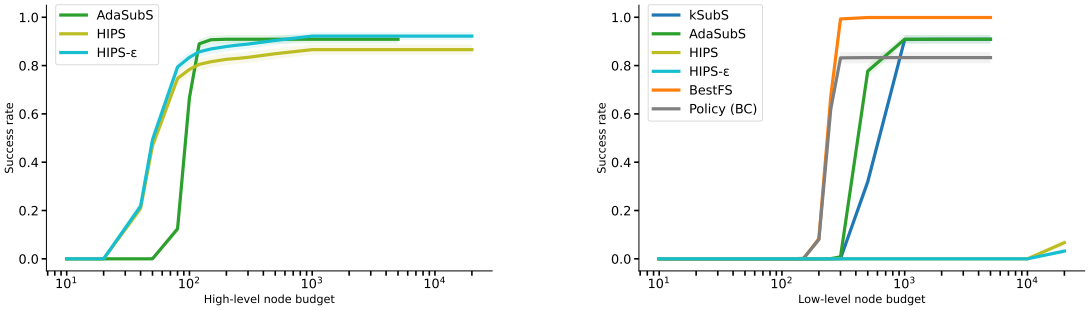


Figure 40: A comparison of high-level and low-level node budgets for considered methods: HIPS, subgoal search methods, and baselines on N-Puzzle. The low-level node budget represents the number of all states that have ever been visited during the search. The bimodal distribution indicates that HIPS methods use disproportionately (over 100x) more low-level nodes than comparable subgoal search methods and baselines. This directly translates to prohibitively slow solving time.

# J Common Pitfalls In Hierarchical Search evaluations

In this study, one of our primary goals is to identify common but often overlooked pitfalls in evaluating hierarchical search methods, which can lead to misleading conclusions. Based on our findings, we propose a set of guidelines that help ensure meaningful and consistent comparisons across different methods. We observed that the nature of hierarchical search makes it easy, whether intentionally or not, to present results in a way that favors certain methods, often without readers being aware. In this section, we present key insights on this issue, with an emphasis on the following evaluation guidelines:

- Report results using a *complete search budget*.
- Include $\rho$-BestFS with a confidence threshold as a baseline.
- Ensure careful tuning of the confidence threshold.
- Use up-to-date code for running experiments.

## J.1 Complete Search Budget

We define the performance metric in terms of *success rate*, which is the percentage of problem instances solved within a specified *complete search budget*. This budget refers to the total number of states visited during the search process. For hierarchical methods, this includes both the subgoals generated and the states visited by the low-level policies connecting those subgoals.

Reporting the *complete search budget* is crucial, as opposed to the *sparse search budget*, which counts only the high-level nodes in the search tree. As discussed in Appendix I, Kujanpää et al. (2023a) rely on the sparse search budget for their evaluations. This creates a misleading impression that HIPS outperforms low-level baselines, while in reality, it requires significantly more computational effort to solve the same problems.

To illustrate this issue, consider a simple environment where an agent must navigate a 100x100 empty room to reach a goal on the opposite side. In this case, a hierarchical method may require only a single subgoal – directly corresponding to the goal state – while a low-level method, even if following the optimal path, would require at least 100 steps. A sparse search budget would misleadingly indicate that the hierarchical method solves the task in one step, while the low-level approach requires 100 steps, implying a 100x higher cost. However, both methods traverse the same path, making this comparison inaccurate. Using the *complete search budget*, both methods would be assigned the same cost, providing a much more meaningful comparison.

This issue arises in practical settings as well. Figure 42 compares subgoal methods and low-level BestFS on the Sokoban environment. The dashed line represents the same runs but evaluated with the sparse search budget instead of the complete search budget. For BestFS, both budget measures are equivalent. The figure clearly demonstrates that while kSubS and $\rho$-BestFS visit a similar number of states to solve an instance, the sparse search budget falsely amplifies the difference between the two methods.

## J.2 Baselines

A common evaluation practice in hierarchical search studies is to compare hierarchical methods against the search algorithm used as the planner (Czechowski et al., 2021; Zawalski et al., 2023; Kujanpää et al., 2023a;b). While this is generally a good approach, it is critical to ensure that baseline methods are properly tuned to allow for fair comparisons.

Our study shows that the most effective low-level method is $\rho$-BestFS with a confidence threshold. This simple greedy search often performs significantly better than other low-level methods and, in some cases, is competitive with subgoal methods. However, if we were to follow prior works such as (Czechowski et al., 2021; Zawalski et al., 2023) and restrict our comparisons to variants of BestFS that select a fixed number of actions in each node expansion, without employing a confidence threshold (see Appendix F.1 for detailed definitions and analysis), we would artificially widen the gap between BestFS and subgoal methods. As noted in Appendix F.1, the performance of $\rho$-BestFS is highly sensitive to the confidence threshold, and

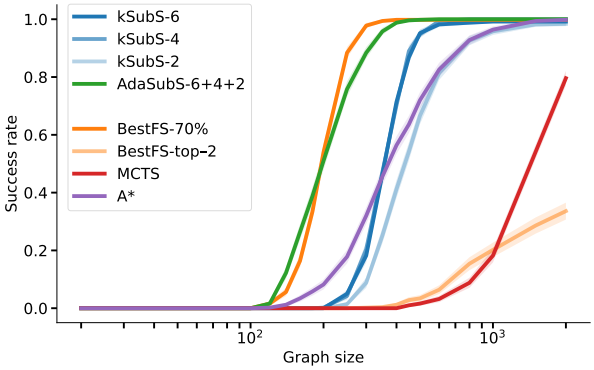


Figure 41: Solving the Rubik's Cube. The light orange line represents the best-performing variant of BestFS that selects a fixed number of actions for each expansion. The solid orange line represents BestFS with actions confidence threshold, which is much more efficient.

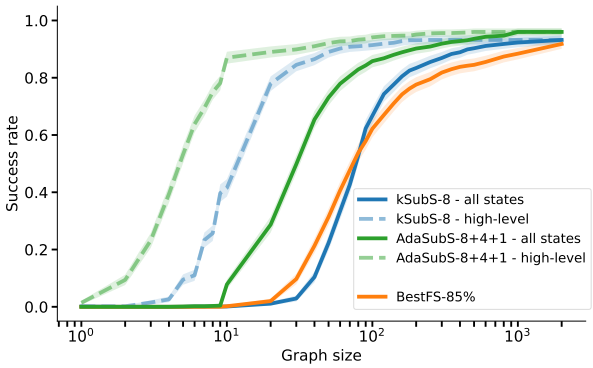


Figure 42: Solving Sokoban. Solid lines correspond to using *complete search budget* as the search tree size metric. Dashed lines correspond to the same runs, but using *sparse search budget* as the search tree size metric. For BestFS, both methods are equivalent.

proper tuning is essential. Nevertheless, we advocate for using $\rho$-BestFS with a confidence threshold as a standard baseline in evaluations of hierarchical methods.

### J.3 Code Quality

While our results generally align with the findings of (Czechowski et al., 2021; Zawalski et al., 2023), we observed some notable differences. Most strikingly, when components were trained on reverse random shuffles of the Rubik's Cube, our models demonstrated significantly better performance. In particular, (Zawalski et al., 2023) reports that both kSubS and AdaSubS substantially outperform $\rho$-BestFS. However, in our experiments, these methods perform similarly, with only minor differences between them (see Figure 43).

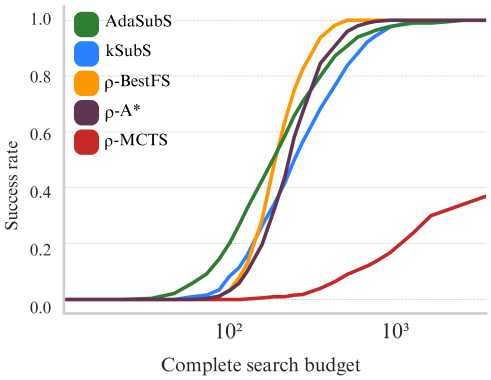


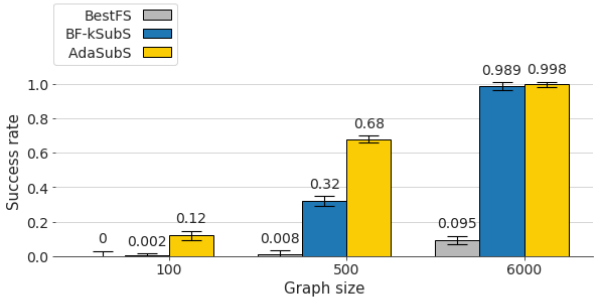


Figure 43: Solving the Rubik's Cube. Components are trained on reverse random shuffles. The left chart present our results, while the right presents results of the same experiment from (Zawalski et al., 2023).

For this study, we re-implemented all algorithms from scratch, using up-to-date libraries and carefully tuning hyperparameters. Our experiments revealed that low-level methods are highly sensitive to the quality of the value function, whereas subgoal-based methods are more resilient (Section 5.2). We hypothesize that the discrepancy in performance compared to (Czechowski et al., 2021; Zawalski et al., 2023) may stem from insufficient training of the value function in their implementation, leading to the observed performance gap.

Using the original implementations of kSubS and AdaSubS, which is a common practice, would replicate the same limitation. This shows the importance of re-implementing algorithms independently and carefully tuning their components, ensuring that evaluations are not biased by potential shortcomings in the original implementations.

## K Proof Of The Search Advancement formula

**Theorem 3** (Search advancement formula, complete statement)**.** *Let $g_k : S \to \mathcal{P}(S)$ be a stochastic $k$-subgoal generator that, given a state $s \in S$ samples a set of $b$ subgoals $\{s_i\}$ such that the distances $d(s_i, s)$ are independent, uniformly distributed in the interval $[-k; k]$. Let $V : S \to \mathbb{R}$ be a value function with approximation error uniformly distributed in the interval $[-\sigma; \sigma]$.*

*Then, after $n$ iterations of search, the expected total progress toward the goal is:*

$$\mathbb{E}_{Adv} = \frac{nb}{4\sigma k} \int_{-k}^{k} x \left( \int_{-\sigma}^{\sigma} \tilde{u}(x+h)^{b-1} \mathrm{d}h \right) \mathrm{d}x, \tag{3}$$

*where $\tilde{u}(x)$ is CDF of the sum of two uniform variables $U(-k,k)+U(-\sigma,\sigma)$. Additionally, if we approximate that sum as $U(-k-\sigma, k+\sigma)$, we get*

$$\mathbb{E}_{Adv} \approx \frac{n\left((k+\sigma)^b(bk^2+bk\sigma-2k\sigma-2\sigma^2)+\sigma^b(2k\sigma+bk\sigma+2\sigma^2)-k^b(bk^2)\right)}{(b+1)(b+2)k\sigma(k+\sigma)^{b-1}} \tag{4}$$

*Proof.* Let $A_1, \ldots, A_b$ be independent and identically distributed (i.i.d.) random variables sampled from $U(-k,k)$, and let $B_1, \ldots, B_b$ be i.i.d. random variables sampled from $U(-\sigma,\sigma)$. Denote the CDF of the sum $A_i + B_i$ as $\tilde{u}(x)$, and its corresponding probability density function (PDF) as $p(x) = \tilde{u}'(x)$. Let $I = \arg\max_i(A_i + B_i)$.

We now define the cumulative likelihood of selecting the largest sum among the subgoals:

$$CLS(x) = \mathbb{P}\left(\forall_{1 \le i \le b}\, A_i + B_i < x\right).$$

Since the $A_i$'s and $B_i$'s are independent, it follows that $CLS(x) = \tilde{u}(x)^b$, which represents the cumulative distribution of the largest sum $A_i + B_i$. Differentiating this expression gives the PDF of the largest sum:

$$PLS(x) = CLS'(x) = b \cdot \tilde{u}(x)^{b-1} \cdot p(x).$$

Now, consider the event that $A_I = x$, which is equivalent to the event that the maximum $\max_i(A_i + B_i) = x + h$ for some $h \in [-\sigma, \sigma]$ and $B_I = h$. Given that $\max_i(A_i + B_i) = x + h$, there are $p(x+h) \cdot 4\sigma k$ possible values of $B_I$, since $A_I \in [-k, k]$ and $B_I \in [-\sigma, \sigma]$. Therefore, the PDF of this variable is

$$q(x) = \int_{-\sigma}^{\sigma} \frac{PLS(x+h)}{p(x+h) \cdot 4\sigma k}\, \mathrm{d}h = \int_{-\sigma}^{\sigma} \frac{b \cdot \tilde{u}(x+h)^{b-1}}{4\sigma k}\, \mathrm{d}h.$$

Thus, the expected value of $A_I$, which represents the progress in each step, is given by

$$\mathbb{E}[A_I] = \int_{-k}^{k} x q(x)\, \mathrm{d}x = \frac{b}{4\sigma k} \int_{-k}^{k} x \left( \int_{-\sigma}^{\sigma} \tilde{u}(x+h)^{b-1}\, \mathrm{d}h \right) \mathrm{d}x.$$

If we model the search process as advancing to the best subgoal in each iteration, the total expected progress after $n$ iterations is

$$\mathbb{E}_{Adv} = n\mathbb{E}[A_I] = \frac{nb}{4\sigma k} \int_{-k}^{k} x \left( \int_{-\sigma}^{\sigma} \tilde{u}(x+h)^{b-1}\, \mathrm{d}h \right) \mathrm{d}x.$$

Finally, by approximating the PDF $p(x) \approx \frac{1}{2k+2\sigma} \mathbb{1}_{[-k-\sigma, k+\sigma]}$, and substituting this approximation into the previous expression, we arrive at the closed-form approximation:

$$\mathbb{E}_{Adv} \approx \frac{n\left((k+\sigma)^b(bk^2+bk\sigma-2k\sigma-2\sigma^2)+\sigma^b(2k\sigma+bk\sigma+2\sigma^2)-k^b(bk^2)\right)}{(b+1)(b+2)k\sigma(k+\sigma)^{b-1}}.$$

□

## L Proof Of The Densification Of The Action Space Theorem

In Section 5.3, we showed experimentally that both in the mathematical INT environment and Rubik's Cube with multiplied action space the advantage of subgoal methods is significant. We attributed those benefits to the ability of subgoal methods to use states as actions and the reduced diversity in low-level search. And indeed, we can prove in general that as the action space gets more complex, the diversity of top actions drops.

To give an illustrative example, in the Rubik's Cube experiment, to model the increasingly complex action space, for an arbitrary state we can view the training data as a ground-truth density function $f$ over an interval $[0, 1]$, that is split evenly between the actions (i.e. into 12 intervals of length 1/12). Then, we can define arbitrarily dense action spaces $A_n$ consisting of $n$ points distributed evenly in the domain. For instance, $A_{12}$ corresponds to the standard Rubik's Cube action space, while $A_{1200}$ corresponds to the variant multiplied 100 times. Our theorem confirms that the actions selected by the policy gets less diverse as the complexity of the action space increases, up to the extreme of converging to a single point as $n$ approaches infinity. In practice, it is even more general, since the data-driven action distribution $f$ may also model smooth interpolation between actions.

While this is rather intuitive when the learned distributions are perfect, it may seem that approximation errors, induced both by the limited training data and the policy network can actually improve diversity. We show that the result holds even in presence of arbitrarily large approximation errors, which is a bit counter-intuitive.

Formally, the theorem is as follows:

**Theorem 4** (Densification of the action space)**.** *Fix any state $s$ from the state space $S$. Let $f : A \to [0, 1]$ be the action distribution induced by the data-collecting policy for the state $s$. Assume that $f$ is continuous and has a unique maximum. For clarity, assume $A = [0, 1]$.*

*Consider a sequence of increasingly dense discrete action spaces $A_n := \{i/n\}_{i=0}^{n} \subset A$. Let $\rho_n : S \times A_n \to [0, 1]$ be a family of policies that learn the distribution $f|_{A_n}$ over actions, with uniform approximation error $U(-E, E)$, where $E \in \mathbb{R}_+$. Let $r_n$ be the range of the top $K$ actions according to the probabilities estimated by $\rho_n$. Then*

$$\lim_{n\to\infty} \mathbb{E}[r_n] = 0.$$

Intuitively, this theorem states that as the action space become more dense and complex, the actions sampled for search become increasingly less diverse, which strongly impedes successful planning. Note that this analysis is strictly more general than the experiment in Section 5.3 with the Rubik's Cube environment, where we simply copied the available actions. Here we model the complexity by adding dense intermediate actions, which leads to a similar conclusion.

While we assume a one-dimensional action domain for clarity, it is straightforward to generalize the proof to cover arbitrarily high-dimensional action spaces.

Firstly, we shall prove the following key lemma.

**Lemma 1.** *Let $f : [0, 1] \to \mathbb{R}$ be a continuous function with a unique maximum. Let $\{a_n\}$ be a partition of the interval $[0, 1]$ into $n$ uniformly spaced points, i.e., $a_{n,i} = \frac{i}{n}$ for $i = 0, 1, \ldots, n$. Define $e_{n,i}$ as i.i.d. samples from a uniform distribution $U(-E, E)$. For a fixed $n$, let $r_n \in \mathbb{R}$ denote the smallest interval length such that the points in $\{a_n\}$ corresponding to the top $K$ values of $f(a_{n,i}) + e_{n,i}$ are contained within this interval. Then*

$$\lim_{n\to\infty} \mathbb{E}[r_n] = 0.$$

*Proof.* Define $p_{n,i,k}$ as the probability that $f(a_{n,i}) + e_{n,i}$ is the $k$-th highest value among all points in $\{a_n\}$. Let $m$ be the unique point such that $f(m)$ is maximal. Without loss of generality, we may assume that $m = 0$.

Let $d_{n,k}$ denote the expected distance of the $k$-th highest point from 0, expressed as

$$d_{n,k} := \sum_{i=0}^{n} p_{n,i,k} a_{n,i}.$$

For sufficiently large $n$, it holds that $r_n \leq d_{n,1} + \ldots + d_{n,K} \leq K d_{n,K}$. Thus, it suffices to prove that $\lim_{n\to\infty} d_{n,K} = 0$.

Fix $\alpha \in (0,1)$ such that $f(a_{n,\alpha n}) \geq f(a_{n,\alpha' n})$ for each $\alpha' > \alpha$. Since $f$ is continuous and $m = 0$ is the unique maximum of $f$, there exist such $\alpha$ arbitrarily close to 0. Let $q_{n,\alpha}$ be the probability that $f(a_{n,\alpha n}) + e_{n,\alpha n}$ is among the top $K$ values. Since $m$ is a unique maximum, there exists $0 < \beta < \alpha$ such that $f(a_{n,\beta n}) > f(a_{n,\alpha n})$. Therefore, if at least $K$ points $a_{n,i}$ with $i/n < \beta$ satisfy $e_{n,i} > E - (f(a_{n,\beta n}) - f(a_{n,\alpha n}))$, then $f(a_{n,\alpha n}) + e_{n,\alpha n}$ cannot be among the top $K$. The probability of this event is a strict upper bound on $q_{n,\alpha}$.

The events $e_{n,i} > E - (f(a_{n,\beta n}) - f(a_{n,\alpha n}))$ are pairwise independent, each occurring with probability

$$c := \frac{f(a_{n,\beta n}) - f(a_{n,\alpha n})}{2E} > 0.$$

For sufficiently large $n$, the probability that at most $K$ of the $\beta n$ trials succeed is bounded by

$$1 - K\binom{\beta n}{K}(1-c)^{\beta n}.$$

Using the asymptotic behavior of binomial coefficients and exponential terms, it follows that

$$\lim_{n\to\infty} n^2 q_{n,\alpha} = 0, \tag{5}$$

with convergence that is exponential.

Using the definition of $d_{n,K}$, decompose it as

$$d_{n,K} = \sum_{i=0}^{n} p_{n,i,K} a_{n,i} = \sum_{i=0}^{\alpha n} p_{n,i,K} a_{n,i} + \sum_{i=\alpha n}^{n} p_{n,i,K} a_{n,i}.$$

For $i \geq \alpha n$, since we know that $f(a_{n,\alpha n}) \geq f(a_{n,\alpha' n})$ for each $\alpha' > \alpha$, we can bound $p_{n,i,K}$ by $p_{n,\alpha n,K}$ for sufficiently large $n$. Therefore

$$\sum_{i=\alpha n}^{n} p_{n,i,K} a_{n,i} \leq (1-\alpha) n p_{n,\alpha n,K}.$$

Since $p_{n,\alpha n,K} \leq q_{n,\alpha}$, it follows that

$$(1-\alpha) n^2 p_{n,\alpha n,K} \leq (1-\alpha) n^2 q_{n,\alpha}.$$

According to Equation 5, this term converges to 0.

For $i \leq \alpha n$, observe that $a_{n,i} < \alpha$ and the probabilities $p_{n,i,K}$ sum to at most 1. Thus

$$\sum_{i=0}^{\alpha n} p_{n,i,K} a_{n,i} \leq \alpha.$$

Combining these bounds, we have

$$\lim_{n\to\infty} d_{n,K} \leq \alpha.$$

Since $\alpha > 0$ was an arbitrarily small constant, it follows that $\lim_{n\to\infty} d_{n,K} = 0$.

By the relation $r_n \leq K d_{n,K}$ and the fact that $\lim_{n\to\infty} d_{n,K} = 0$, we conclude that

$$\lim_{n\to\infty} \mathbb{E}[r_n] = 0.$$

□

Now, Theorem 4 is a straightforward implication of Lemma 1, applied to the sequence of policies $\rho_n$ and increasingly dense action spaces $A_n$.